Photochemical Evaluation of the Norrish-type Decomposition of Aldehydes as CO Donors for the Carbonylation of Hydrocarbons

Jasmin Hack[a], Alina Schmitt[a], Maik Seemann[a], Daniel Pech[a], Tianbai Huang[b] and Robert Geitner *[a]

[a] Institute of Chemistry and Bioengineering, Technical University Ilmenau, Weimarer Str. 32, 98693 Ilmenau, Germany

[b] Institute for Physical Chemistry (IPC) and Abbe Center of Photonics, Friedrich Schiller University Jena, Helmholtzweg 4, 07743 Jena, Germany

*e-mail: robert.geitner@tu-ilmenau.de

1. Results Kinetic Fitting

Table S1. Kinetic rate constants extracted by fitting depending on the sacrificial aldehydes and light intensity setting (LI). Values for $k_{1\text{-}9}$ are in 10^{-5} s^{-1}.

Ligand	Substrate	LI	Rep.	k_1	k_2	k_3	k_4	k_5	k_6	k_7	k_{-7}	k_8	k_9
PMe_3	Acetaldehyde	80.5	1	-	-	-	0.3	-	0.1	0.4	48.9	8	$9.4\cdot10^3$
PMe_3	Acetaldehyde	189.5	1	-	-	-	2	-	0.3	$4.0\cdot10^2$	5.9	24	$1.9\cdot10^4$
PMe_3	Acetaldehyde	388.2	1	-	-	-	1.1	-	0.3	29.1	80.9	$4.9\cdot10^2$	$2.2\cdot10^3$
PMe_3	Acetaldehyde	825.1	1	-	-	-	2.2	-	0.5	0.4	$2.3\cdot10^2$	21.2	$1.5\cdot10^3$
PMe_3	Benzaldehyde	80.5	1	0.8	0	0	$1.1\cdot10^3$	0.3	0.1	32.9	6.7	$2.2\cdot10^2$	$4.4\cdot10^3$
PMe_3	Benzaldehyde	80.5	2	0.6	0	0.1	$1.2\cdot10^3$	0.3	0	14.4	$3.6\cdot10^2$	$3.7\cdot10^4$	$1.4\cdot10^3$
PMe_3	Benzaldehyde	80.5	3	0.9	0	0	$1.7\cdot10^6$	0.7	$3.2\cdot10^6$	6.3	$1.3\cdot10^3$	2.8	12
PMe_3	Benzaldehyde	189.5	1	1.4	0	0	$1.3\cdot10^5$	0.9	$1.8\cdot10^5$	0	$2.9\cdot10^5$	47.4	0.6
PMe_3	Benzaldehyde	189.5	2	1.3	0	0.2	79.2	1.3	5.8	0.4	$7.9\cdot10^2$	32.6	0.6
PMe_3	Benzaldehyde	189.5	3	1.6	0	0.1	68.5	1.5	0.1	29.4	$6.7\cdot10^4$	21.7	54.5
PMe_3	Benzaldehyde	388.2	1	2.2	0	0.2	66.6	1.9	0	$1.5\cdot10^3$	$4.7\cdot10^2$	$3.1\cdot10^2$	$1.2\cdot10^5$
PMe_3	Benzaldehyde	825.1	1	12.9	0.1	0.1	$7.7\cdot10^2$	1	36.1	$5.1\cdot10^2$	$1.7\cdot10^2$	$2.0\cdot10^2$	$2.4\cdot10^4$
PMe_3	Cis-4-Hept.	80.5	1	0.2	0	0	$>10^8$	0	1.6	$9.0\cdot10^2$	$8.3\cdot10^2$	0	$>10^8$
PMe_3	Cis-4-Hept.	189.5	1	0.3	0	0	0	0	$1.0\cdot10^3$	$>10^8$	$8.9\cdot10^6$	7.4	$>10^8$
PMe_3	Cis-4-Hept.	388.2	1	1.0	0	0.1	$2.6\cdot10^2$	0	0.1	$1.4\cdot10^3$	$9.2\cdot10^2$	$2.3\cdot10^2$	$4.3\cdot10^4$

PMe_3	Cis-4-Hept.	825.1	1	1.4	0	0.1	0.4	0	1.4	2.8	0.5	$4.7 \cdot 10^3$	$8.8 \cdot 10^6$
PMe_3	CHA	80.5	1	0.5	0.1	0.1	29.5	0.2	3	13.5	$2.8 \cdot 10^2$	$9.2 \cdot 10^2$	$2.1 \cdot 10^4$
PMe_3	CHA	189.5	1	0.6	0.3	0.1	31.5	0.3	0	9.3	8.2	6.2	34.6
PMe_3	CHA	388.2	1	1.3	0.4	0.3	26.6	0.4	2.8	61.4	1.3	7.7	$6.7 \cdot 10^2$
PMe_3	CHA	825.1	1	6.0	1.9	0.9	78.9	0.9	0.3	2.8	14.9	52.4	$3.1 \cdot 10^2$
PMe_3	Octanal	80.5	1	0.3	0	0.2	0.7	0	0	0.4	0.1	$3.2 \cdot 10^5$	$>10^8$
PMe_3	Octanal	189.5	1	0.6	0	0.3	0.6	0	0	$1.1 \cdot 10^2$	$1.5 \cdot 10^2$	0.3	$2.1 \cdot 10^5$
PMe_3	Octanal	388.2	1	1.1	0	0.4	0	0	0	$>10^8$	$>10^8$	0	$>10^8$
PMe_3	Octanal	825.1	1	2.4	0	1.1	0.4	0	0	$1.1 \cdot 10^7$	$>10^8$	$2.1 \cdot 10^3$	$>10^8$
-	Benzaldehyde	80.5	1	2.5	0.1	0.1	$2.9 \cdot 10^2$	0.1	0	38.1	0	$>10^8$	$4.3 \cdot 10^3$
-	Benzaldehyde	189.5	1	6.8	0	0.4	$4.3 \cdot 10^2$	0.1	0.1	$1.6 \cdot 10^2$	0	$7.6 \cdot 10^4$	$1.2 \cdot 10^4$
-	Benzaldehyde	388.2	1	11.3	0	1	$5.9 \cdot 10^2$	0.3	1	18.5	8.2	48.6	$1.2 \cdot 10^3$
-	Benzaldehyde	825.1	1	37.9	0	0.4	0	0.9	1.2	62.5	$1.0 \cdot 10^3$	$6.3 \cdot 10^2$	$1.8 \cdot 10^3$
-	Benzaldehyde	80.5 (glass)	1	1.2	0	0		0	$6.3 \cdot 10^4$	0	$2.0 \cdot 10^5$	0	$>10^8$
-	Benzaldehyde	189.5 (glass)	1	0.9	0	0.1		0	0	3.7	$1.8 \cdot 10^3$	$2.4 \cdot 10^2$	46.8
-	Benzaldehyde	388.2 (glass)	1	2.2	0	0		0	14.3	$2.4 \cdot 10^2$	0	11.9	$1.7 \cdot 10^4$
PMe_3	Benzaldehyde	189.5 (glass)	1	0.5	0	0	$3.7 \cdot 10^7$	0.1	$1.5 \cdot 10^4$	0.1	$2.5 \cdot 10^3$	$1.8 \cdot 10^2$	0.2

2. Reference Experiments

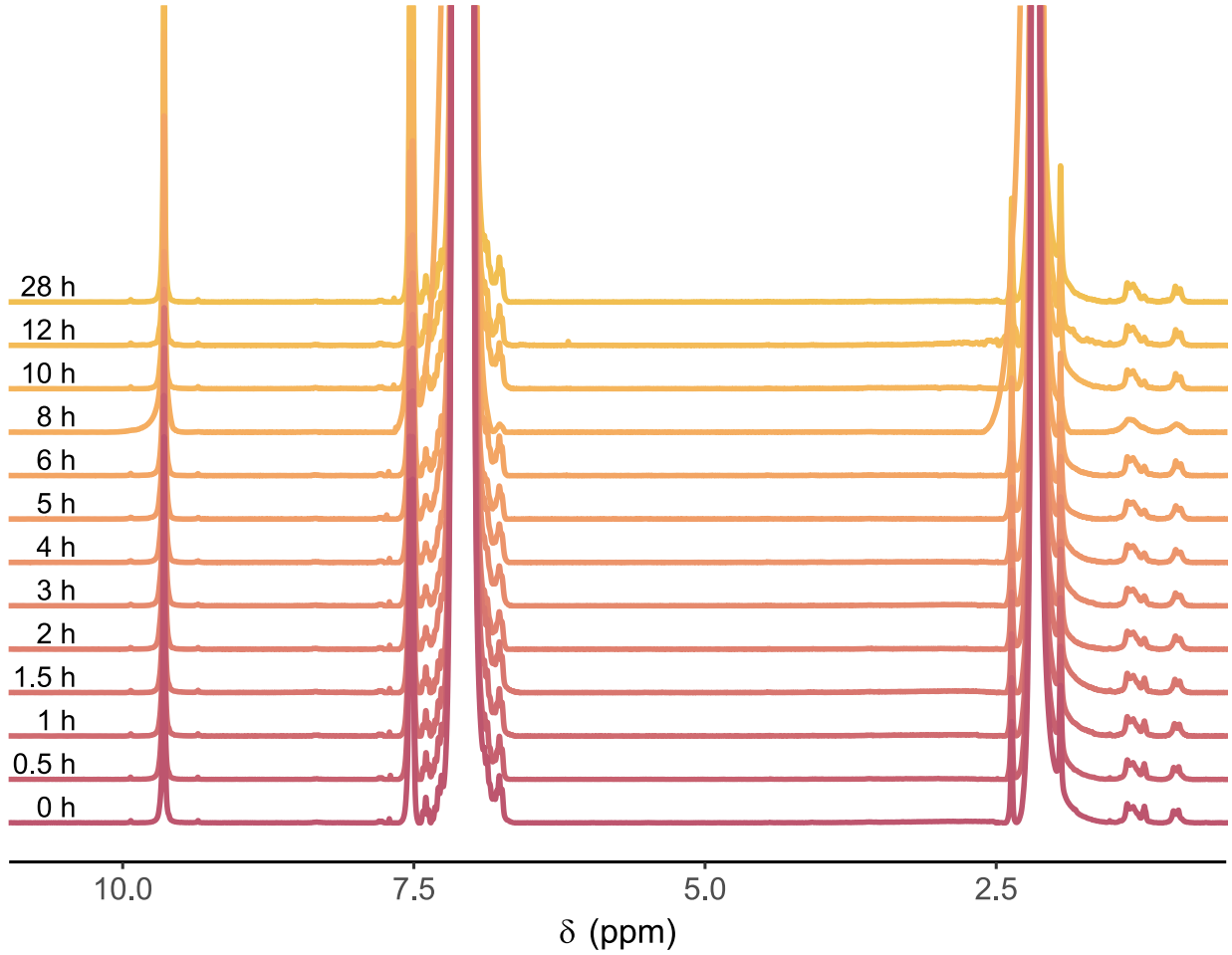

Figure S1. ^{1}H NMR spectra of the thermally driven carbonylation of toluene using benzaldehyde as CO source and [Rh(PMe$_3$)$_2$(Cl)(CO)] as catalyst at 50 °C. No reaction is visible.

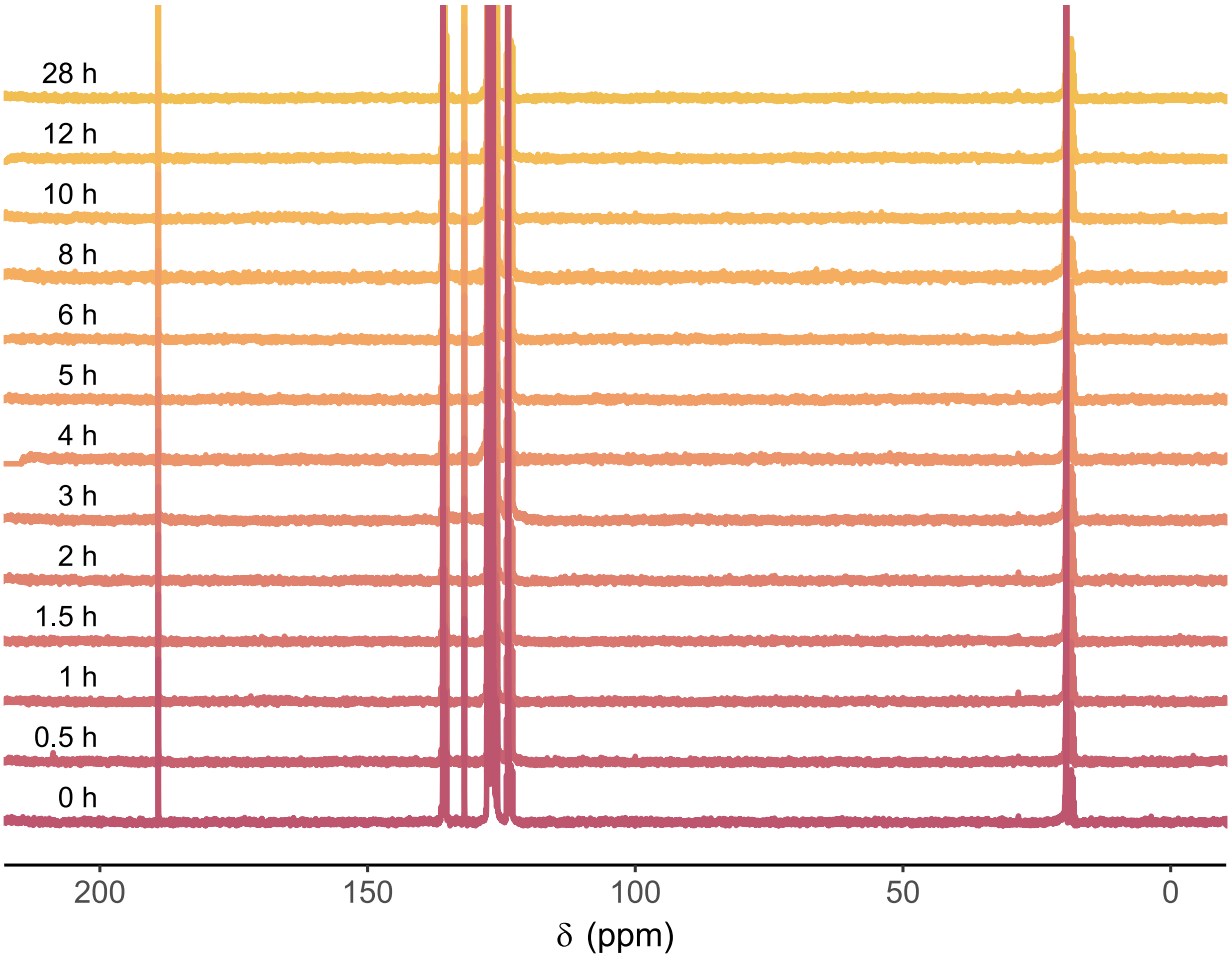

Figure S2. ^{13}C NMR spectra of the thermally driven carbonylation of toluene using benzaldehyde as CO source and $[Rh(PMe_3)_2(Cl)(CO)]$ as catalyst at 50 °C. No reaction is visible.

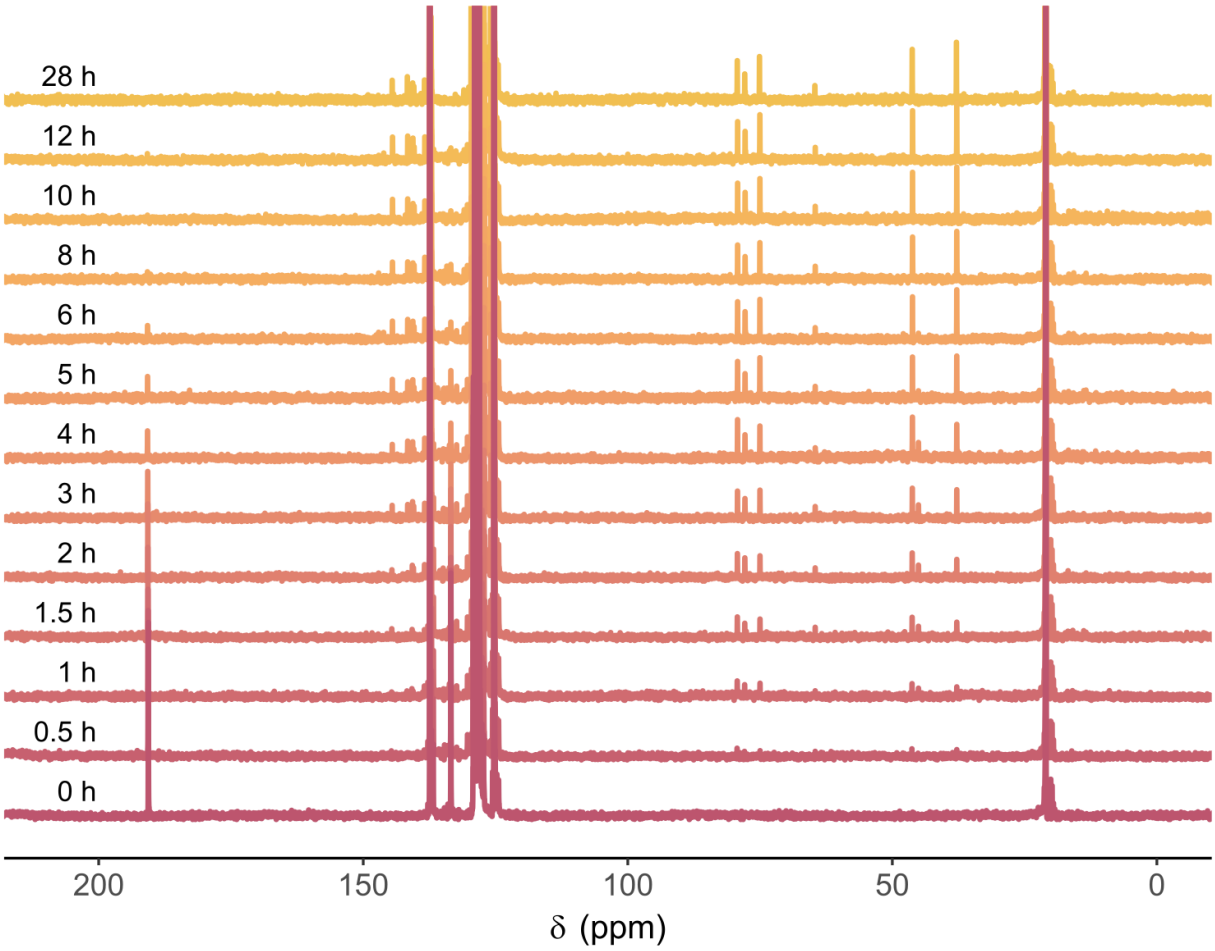

Figure S3. ^{13}C NMR spectra of the photocatalytic carbonylation of toluene using benzaldehyde as CO source and $[Rh(PMe_3)_2(Cl)(CO)]$ as catalyst at a photon flux density of 825.1 µmol m^{-2} s^{-1}.

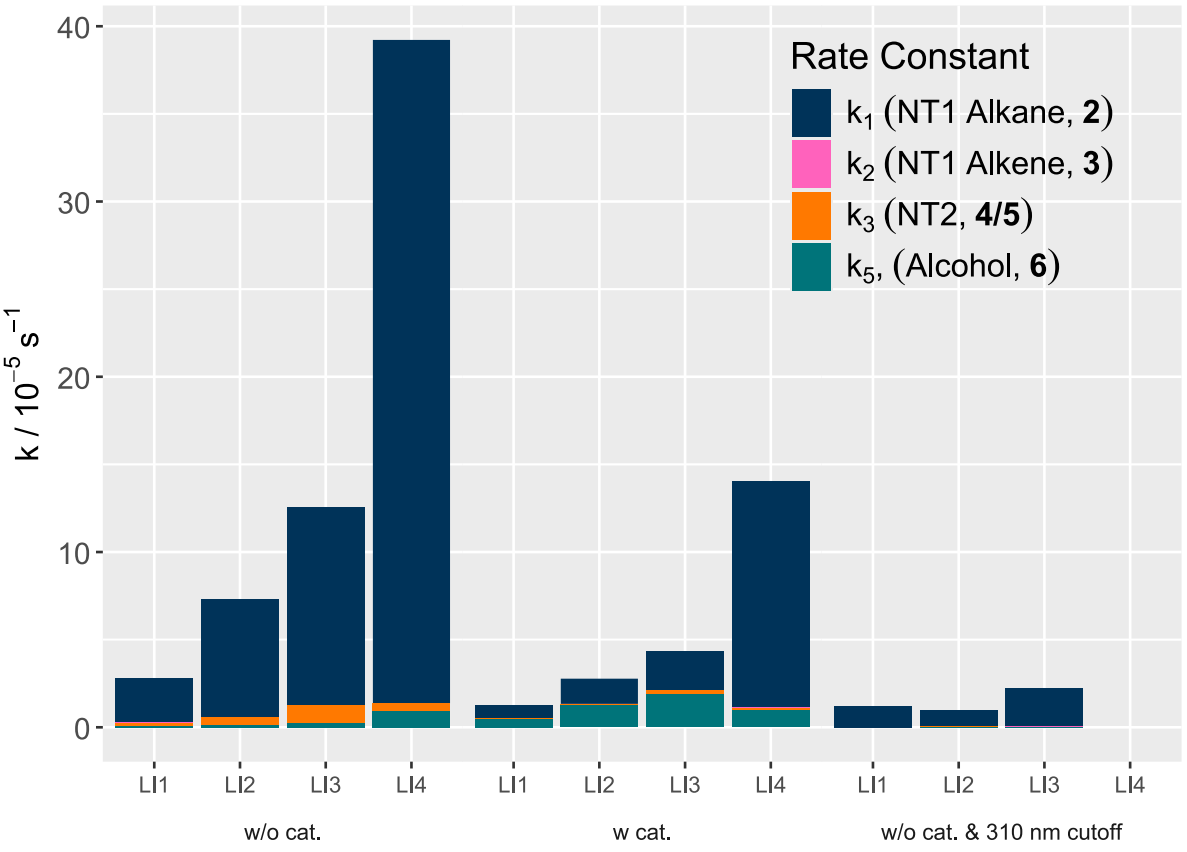

Figure S4. Regular rate constants as extracted by the kinetic fitting procedure for the light-driven decomposition and reaction of benzaldehyde depending on the photon flux density (LI, see **Table S1** for values). Three different reaction conditions (without $[Rh(PMe_3)_2(Cl)(CO)]$, with $[Rh(PMe_3)_2(Cl)(CO)]$ and without $[Rh(PMe_3)_2(Cl)(CO)]$ and an 8 mm window glass) are compared.

3. Results Kinetic Fitting

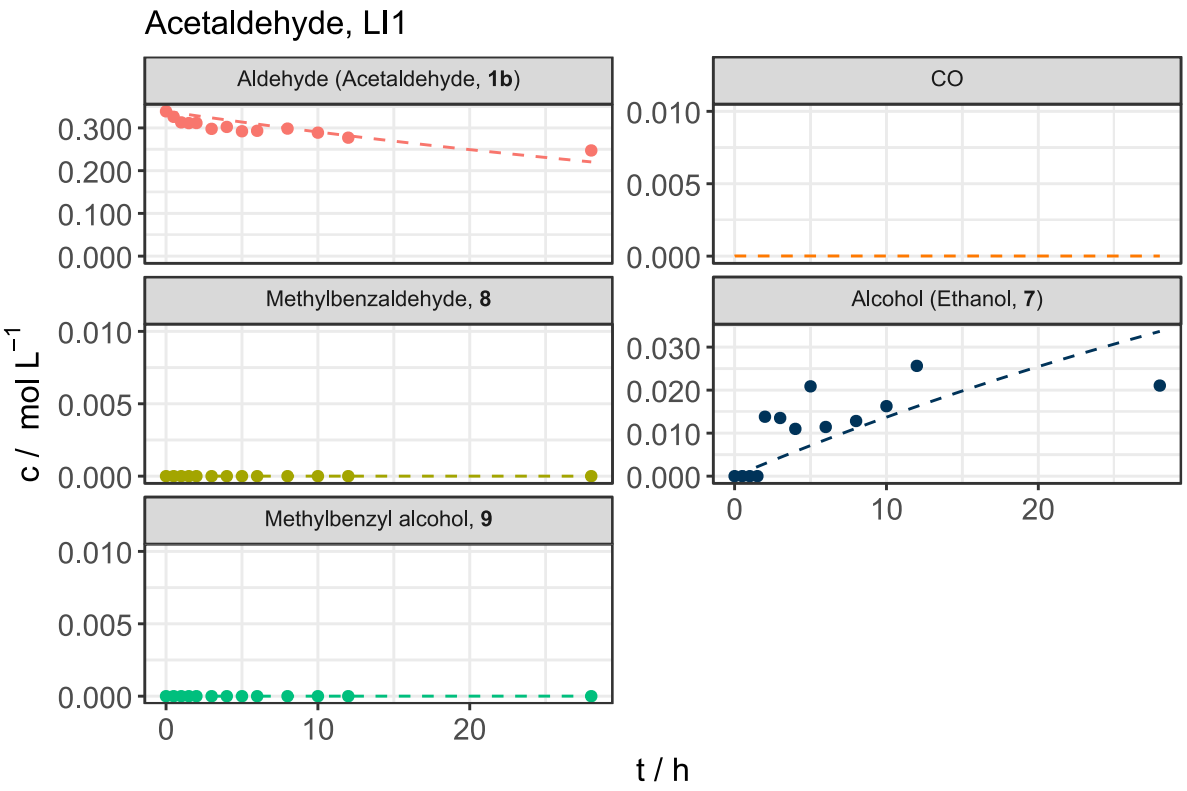

Figure S5. Concentration-time profiles for different species for the light-driven activation of acetaldehyde and the subsequent carbonylation of toluene at a photon flux density of 80.5 µmol m^{-2} s^{-1}.

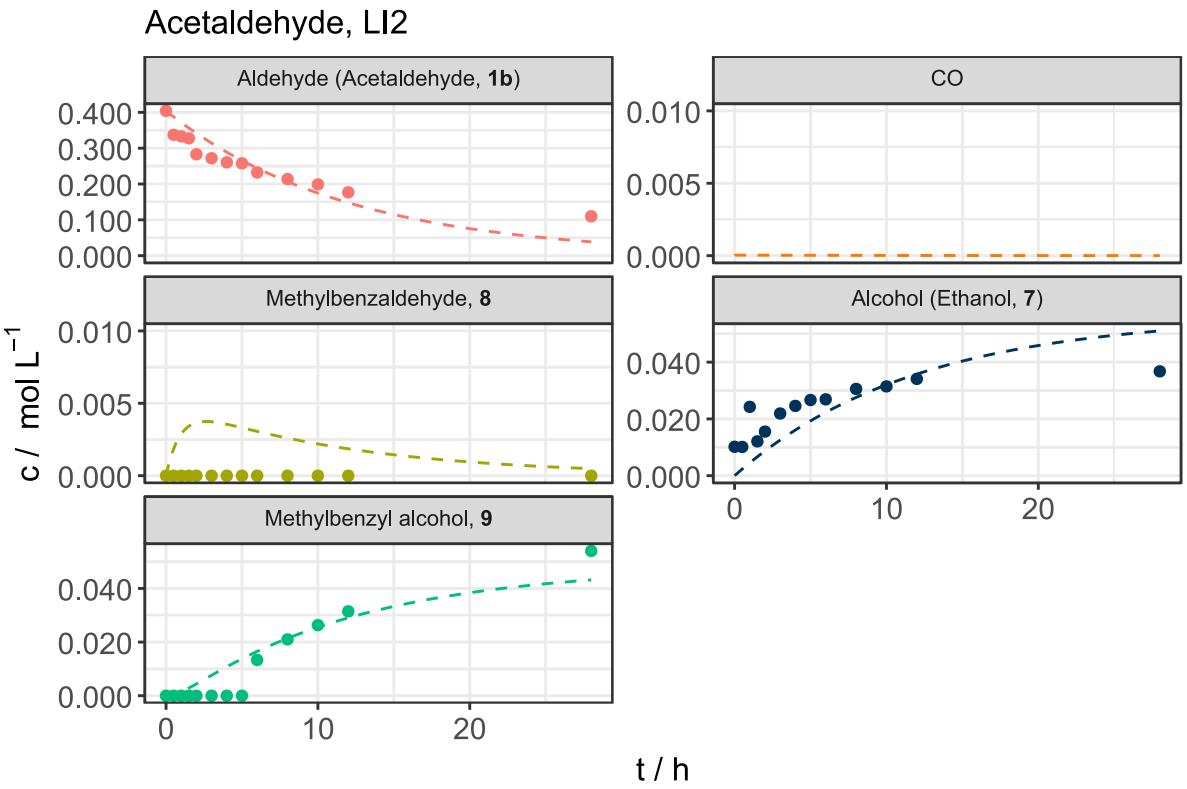

Figure S6. Concentration-time profiles for different species for the light-driven activation of acetaldehyde and the subsequent carbonylation of toluene at a photon flux density of 189.6 µmol m^{-2} s^{-1}.

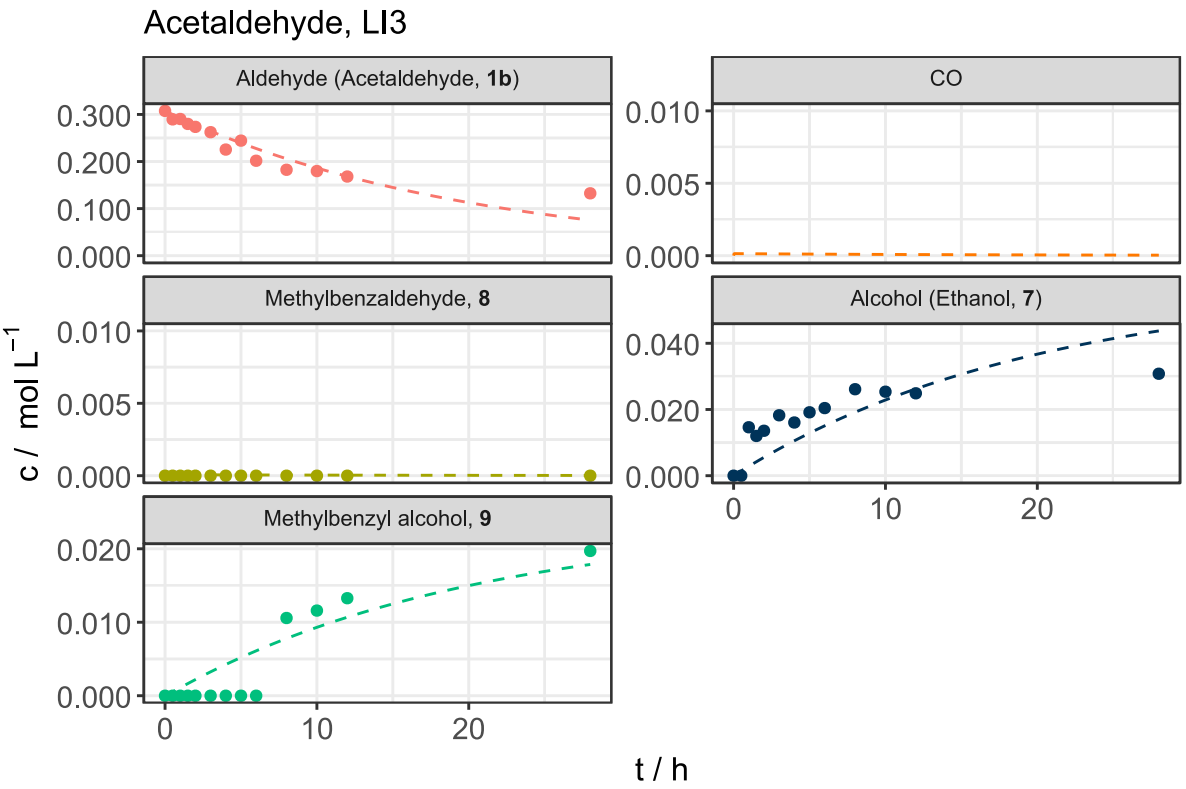

Figure S7. Concentration-time profiles for different species for the light-driven activation of acetaldehyde and the subsequent carbonylation of toluene at a photon flux density of 388.2 µmol m^{-2} s^{-1}.

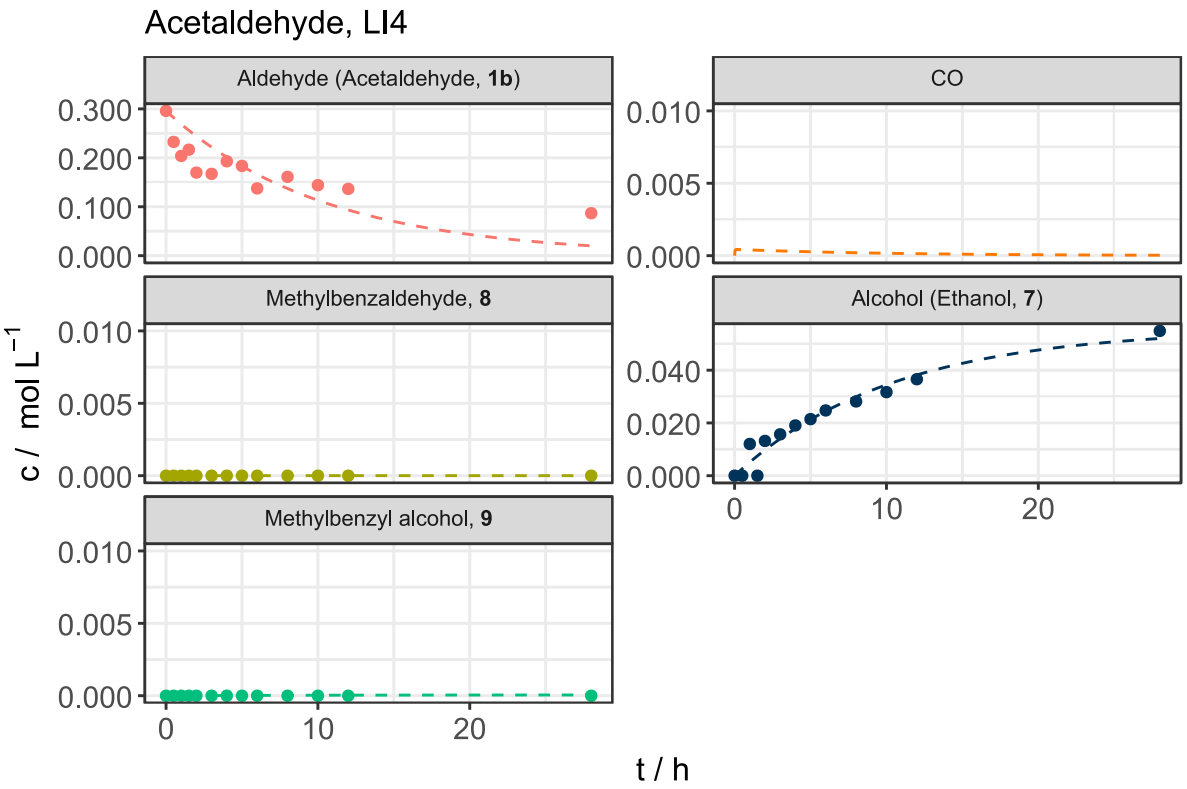

Figure S8. Concentration-time profiles for different species for the light-driven activation of acetaldehyde and the subsequent carbonylation of toluene at a photon flux density of 825.1 µmol m^{-2} s^{-1}.

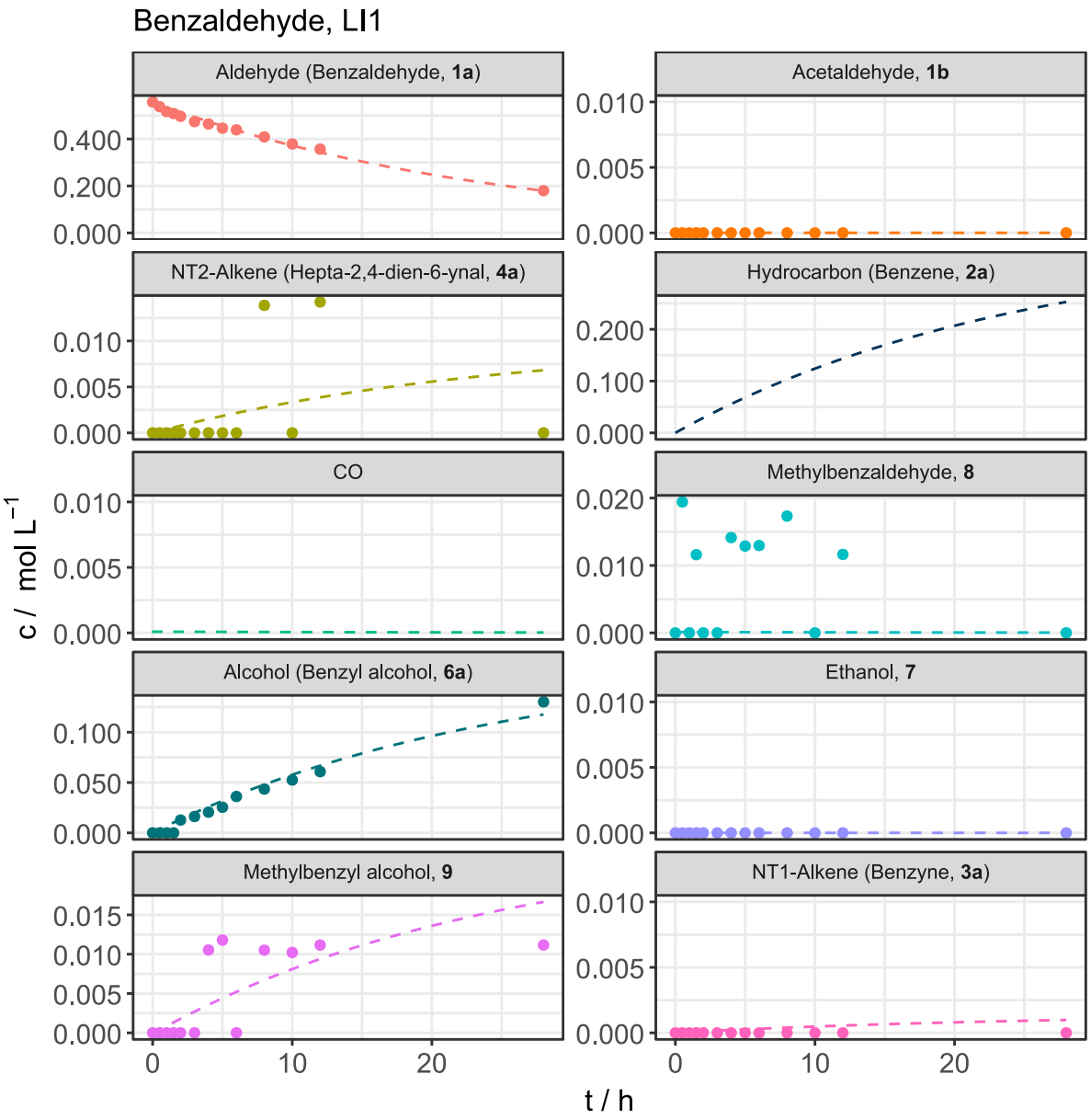

Figure S9. Concentration-time profiles for different species for the light-driven activation of benzaldehyde and the subsequent carbonylation of toluene at a photon flux density of 80.5 µmol m^{-2} s^{-1}.

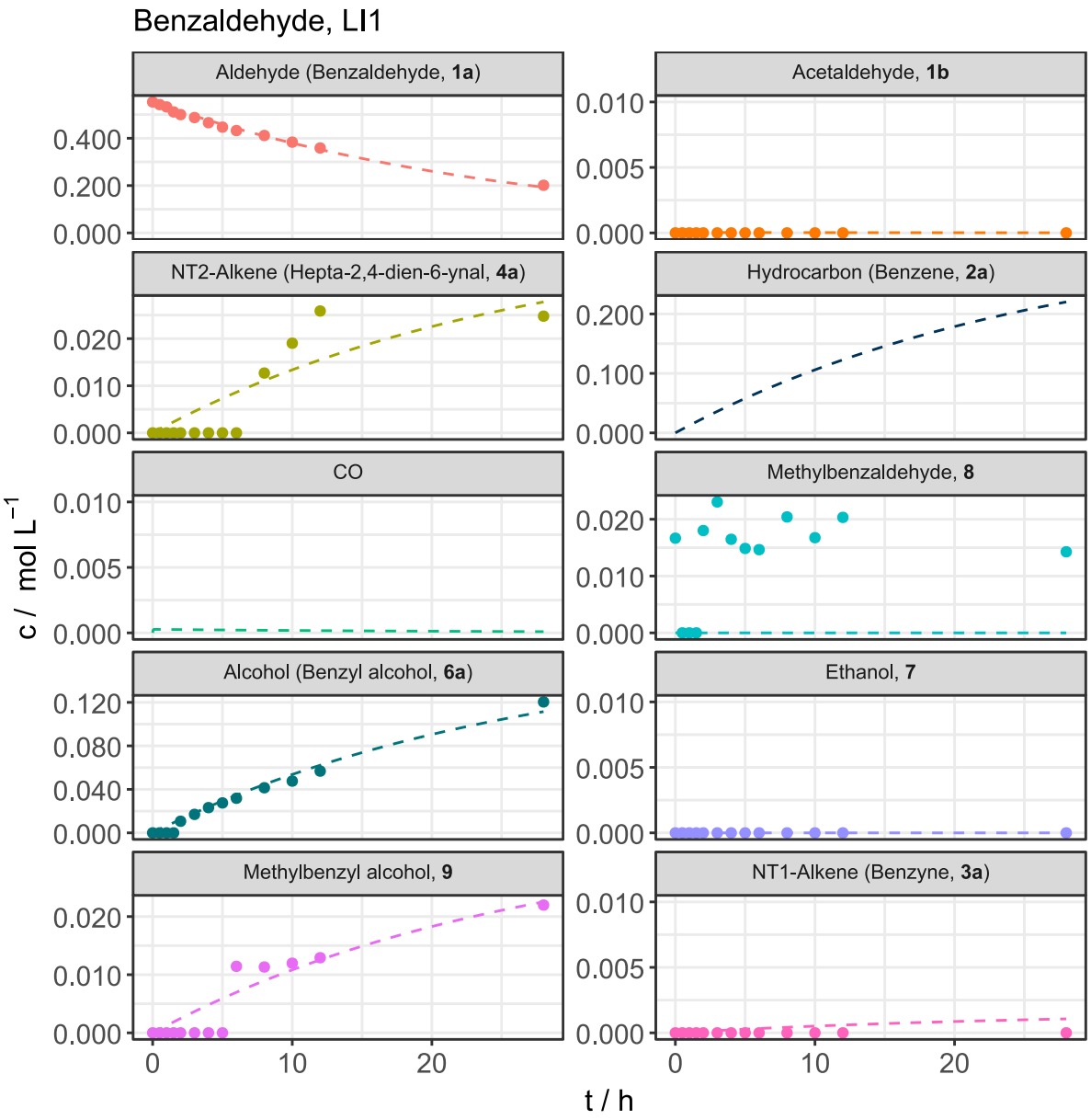

Figure S10. Concentration-time profiles for different species for the light-driven activation of benzaldehyde and the subsequent carbonylation of toluene at a photon flux density of 80.5 µmol m^{-2} s^{-1}.

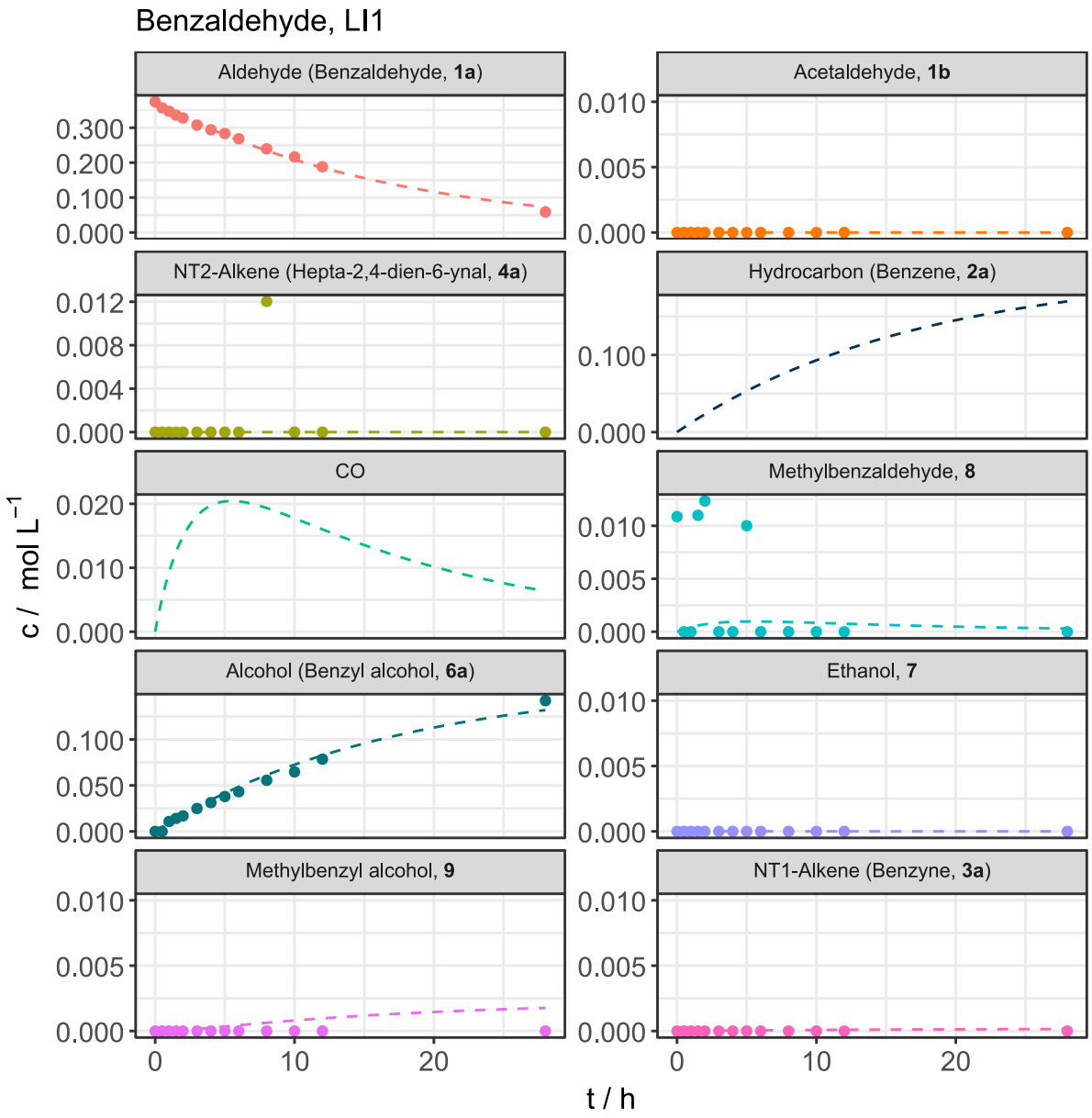

Figure S11. Concentration-time profiles for different species for the light-driven activation of benzaldehyde and the subsequent carbonylation of toluene at a photon flux density of 80.5 µmol m^{-2} s^{-1}.

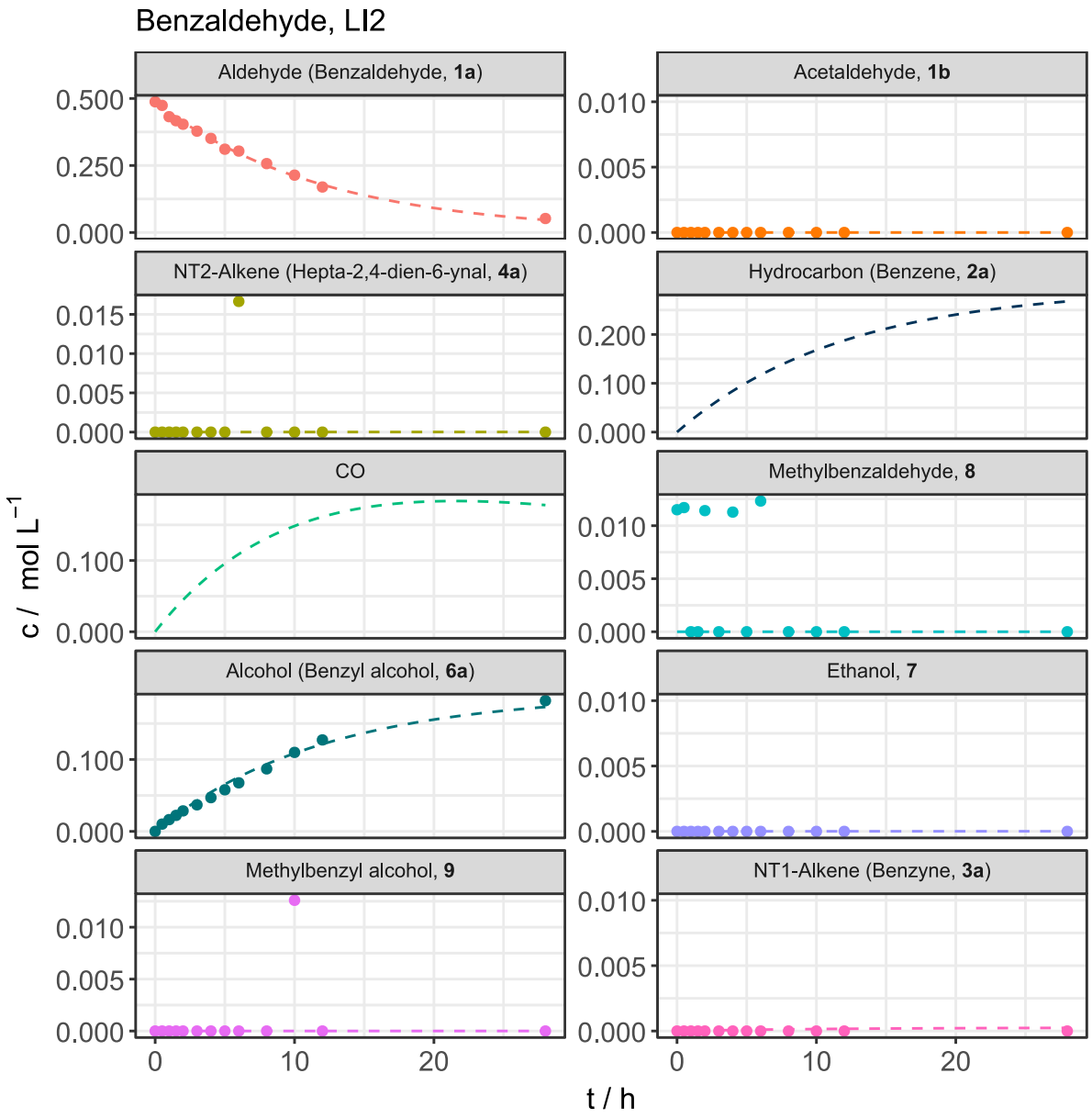

Figure S12. Concentration-time profiles for different species for the light-driven activation of benzaldehyde and the subsequent carbonylation of toluene at a photon flux density of 189.6 µmol m^{-2} s^{-1}.

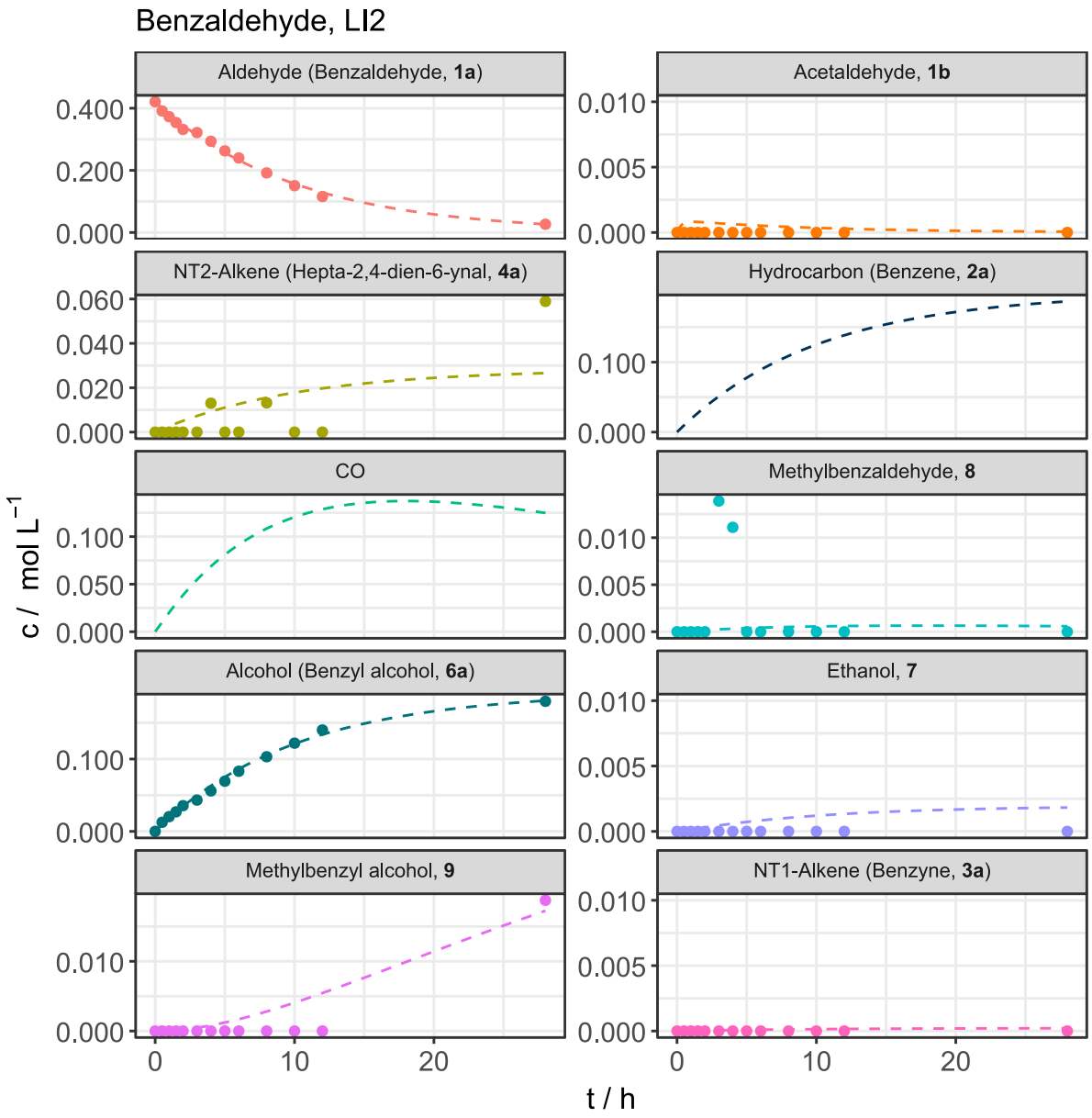

Figure S13. Concentration-time profiles for different species for the light-driven activation of benzaldehyde and the subsequent carbonylation of toluene at a photon flux density of 189.6 µmol m^{-2} s^{-1}.

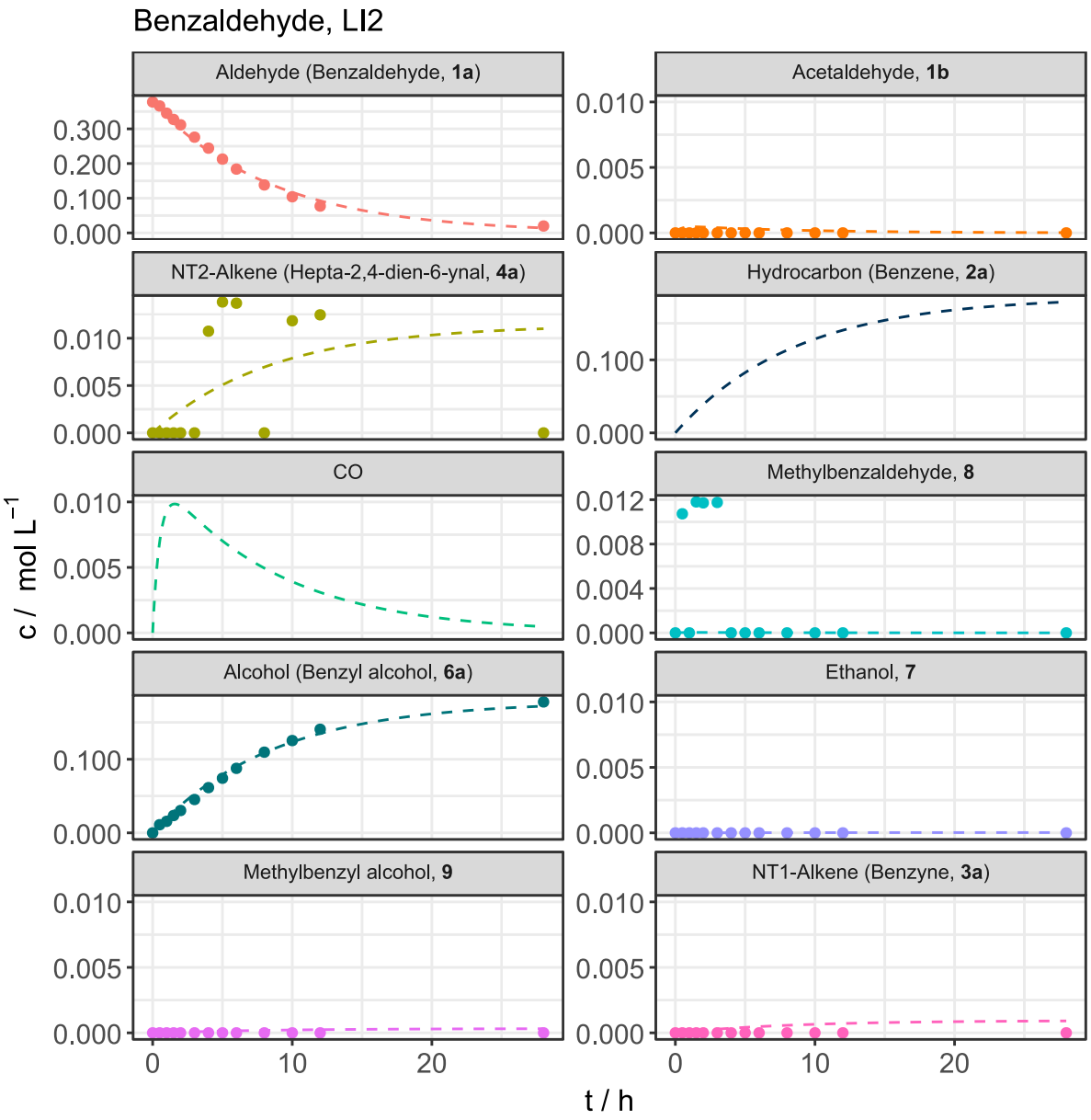

Figure S14. Concentration-time profiles for different species for the light-driven activation of benzaldehyde and the subsequent carbonylation of toluene at a photon flux density of 189.6 µmol m^{-2} s^{-1}.

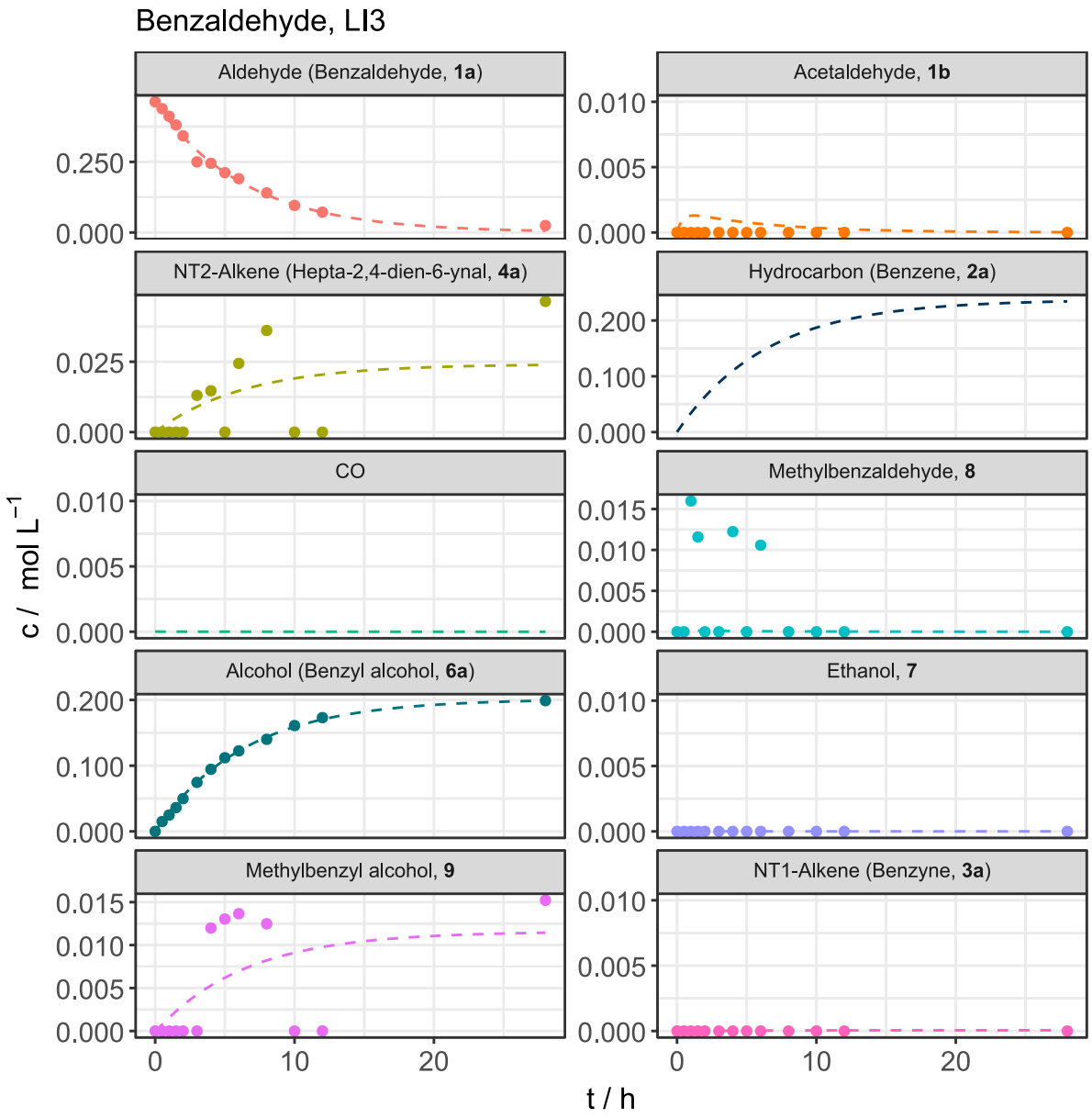

Figure S15. Concentration-time profiles for different species for the light-driven activation of benzaldehyde and the subsequent carbonylation of toluene at a photon flux density of 388.2 µmol m^{-2} s^{-1}.

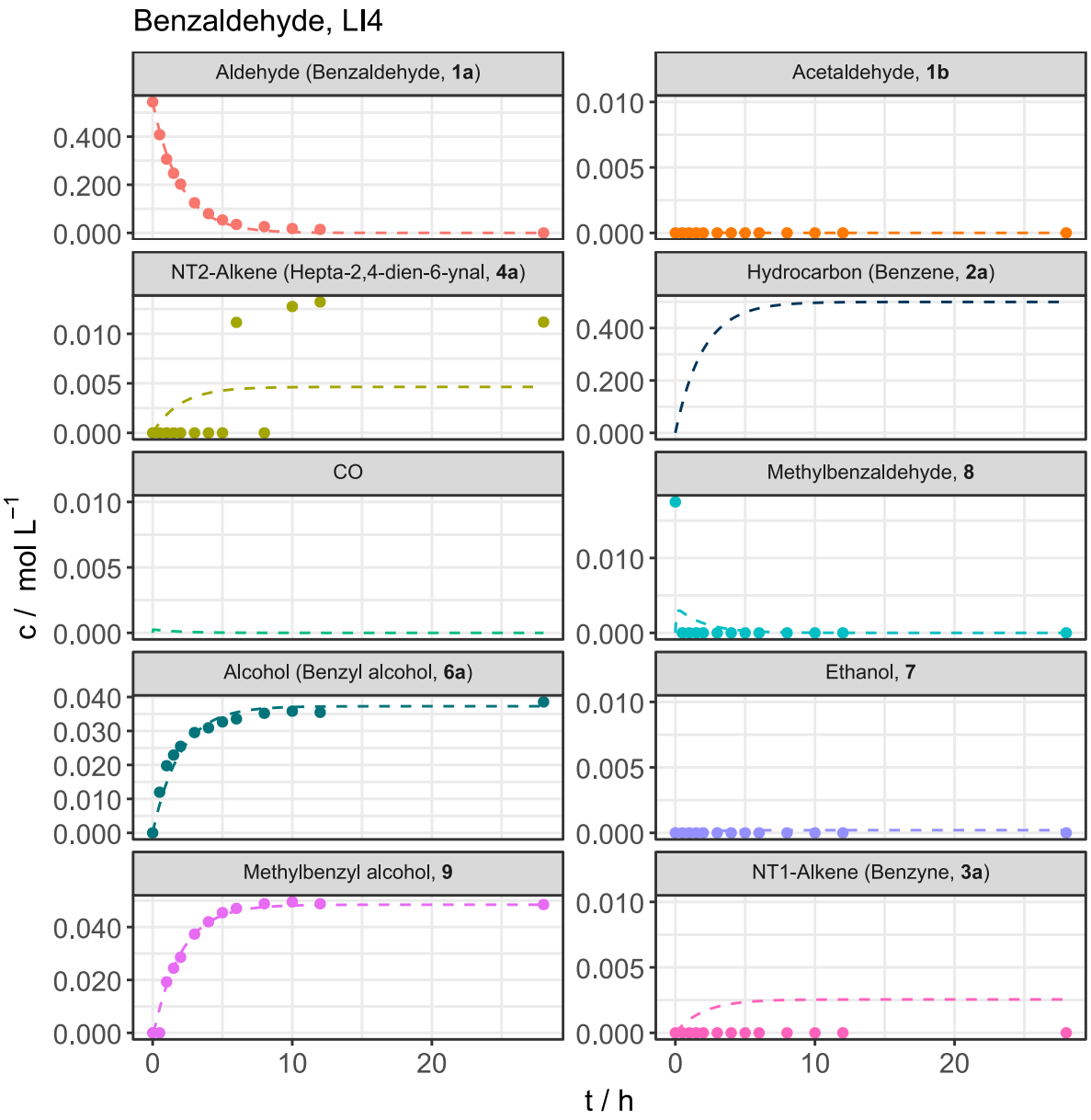

Figure S16. Concentration-time profiles for different species for the light-driven activation of benzaldehyde and the subsequent carbonylation of toluene at a photon flux density of 825.1 µmol m^{-2} s^{-1}.

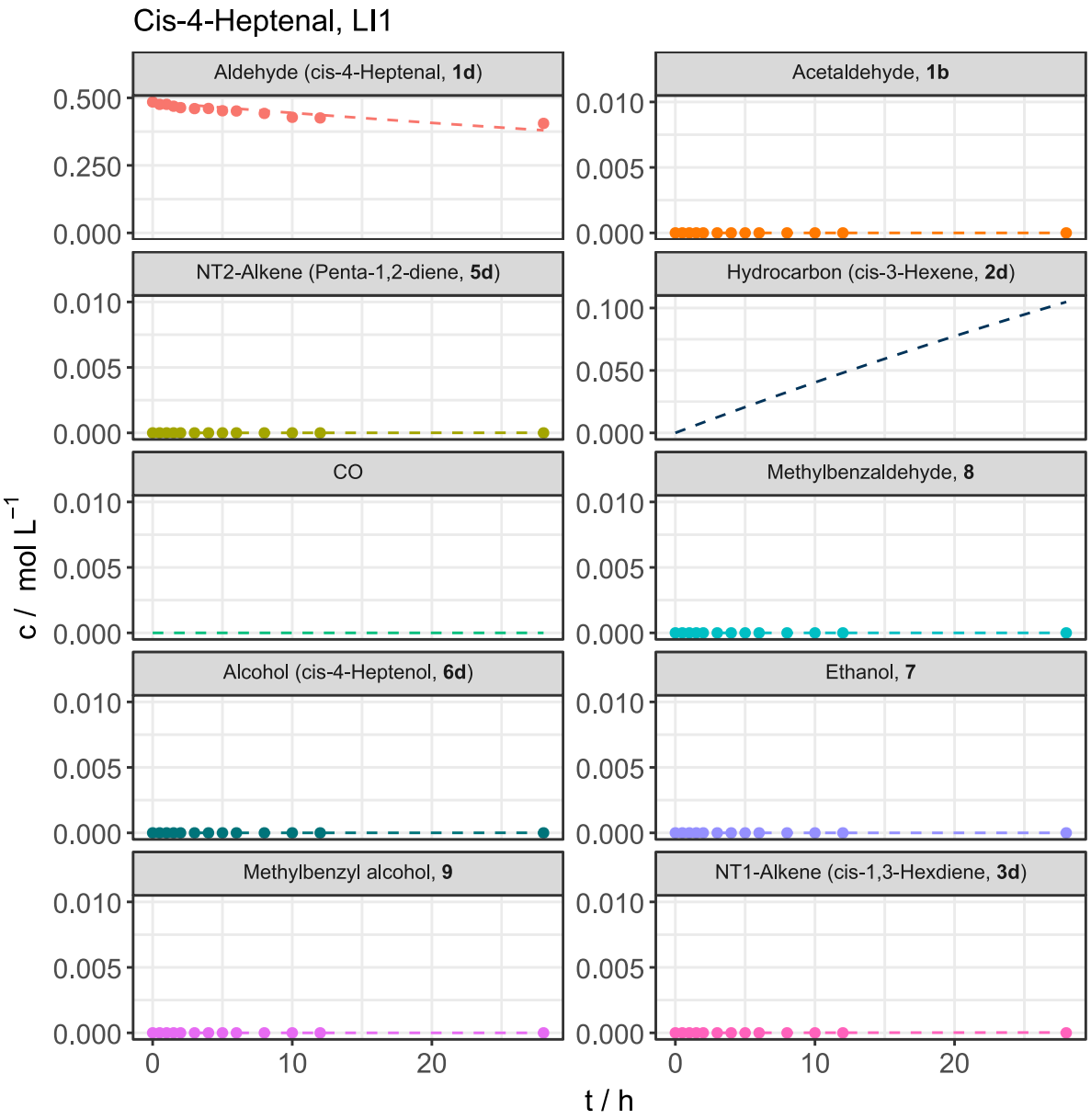

Figure S17. Concentration-time profiles for different species for the light-driven activation of cis-4-heptenal and the subsequent carbonylation of toluene at a photon flux density of 80.5 µmol m^{-2} s^{-1}.

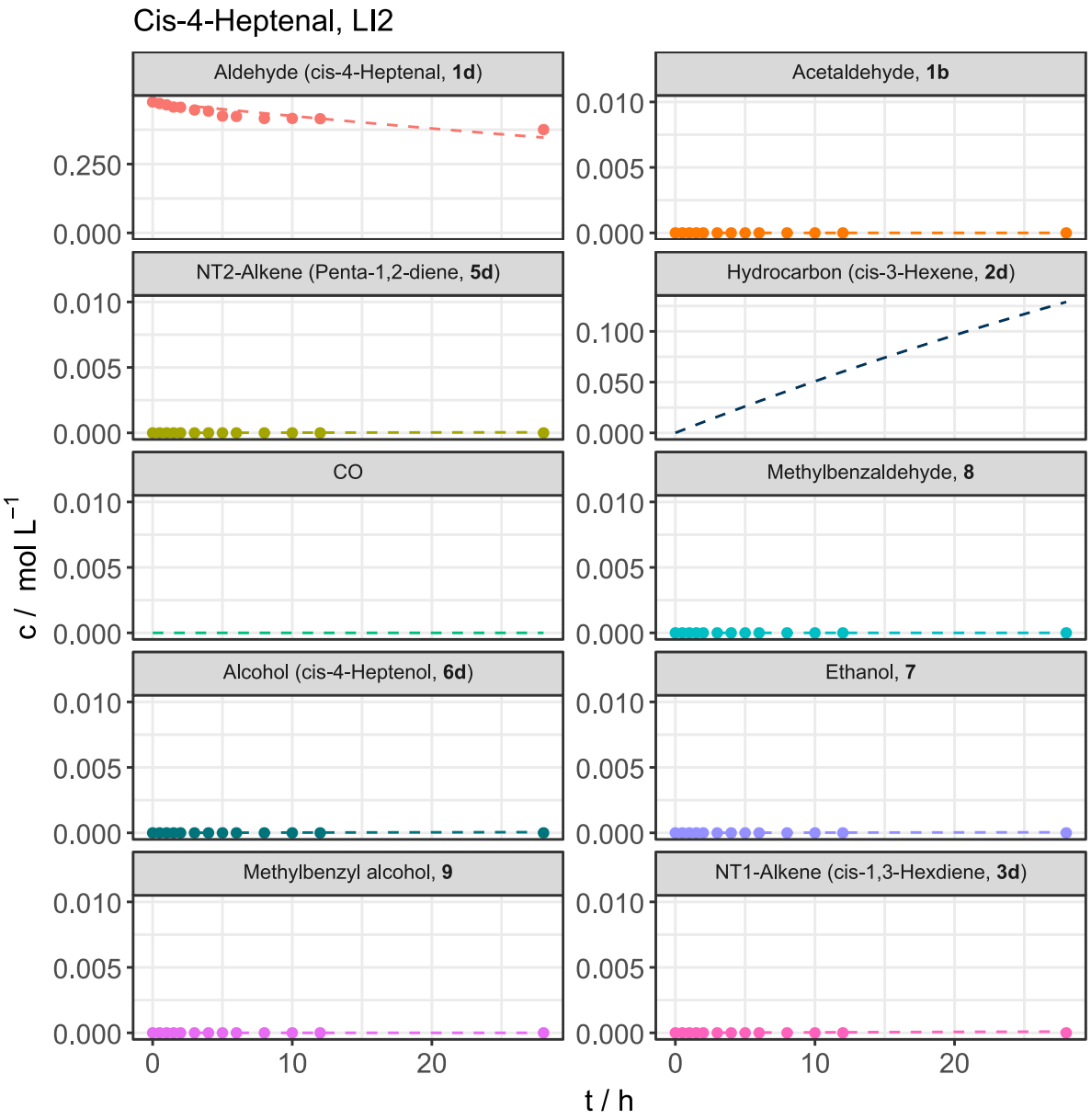

Figure S18. Concentration-time profiles for different species for the light-driven activation of cis-4-heptenal and the subsequent carbonylation of toluene at a photon flux density of 189.6 µmol m^{-2} s^{-1}.

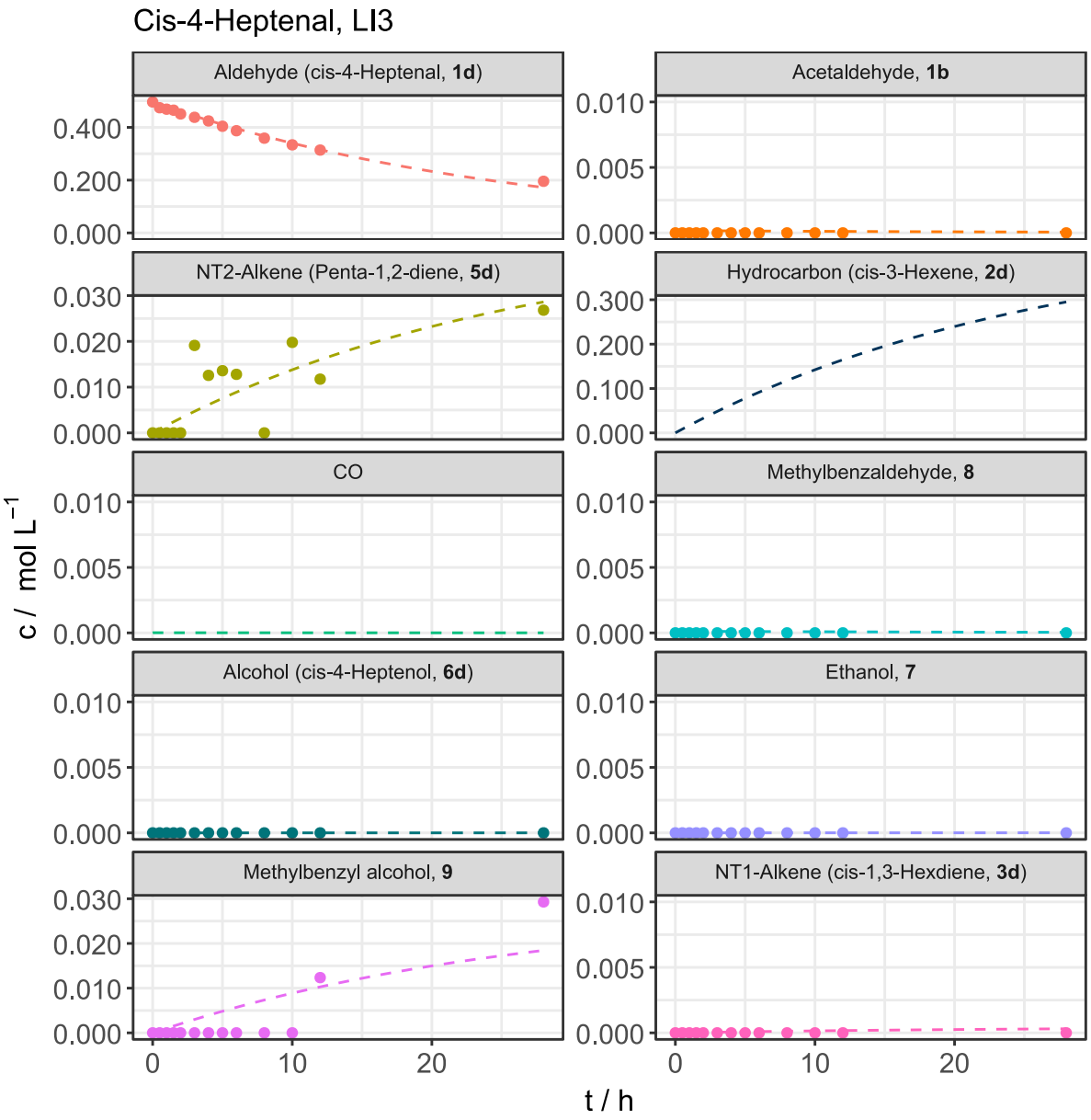

Figure S19. Concentration-time profiles for different species for the light-driven activation of cis-4-heptenal and the subsequent carbonylation of toluene at a photon flux density of 388.2 µmol m^{-2} s^{-1}.

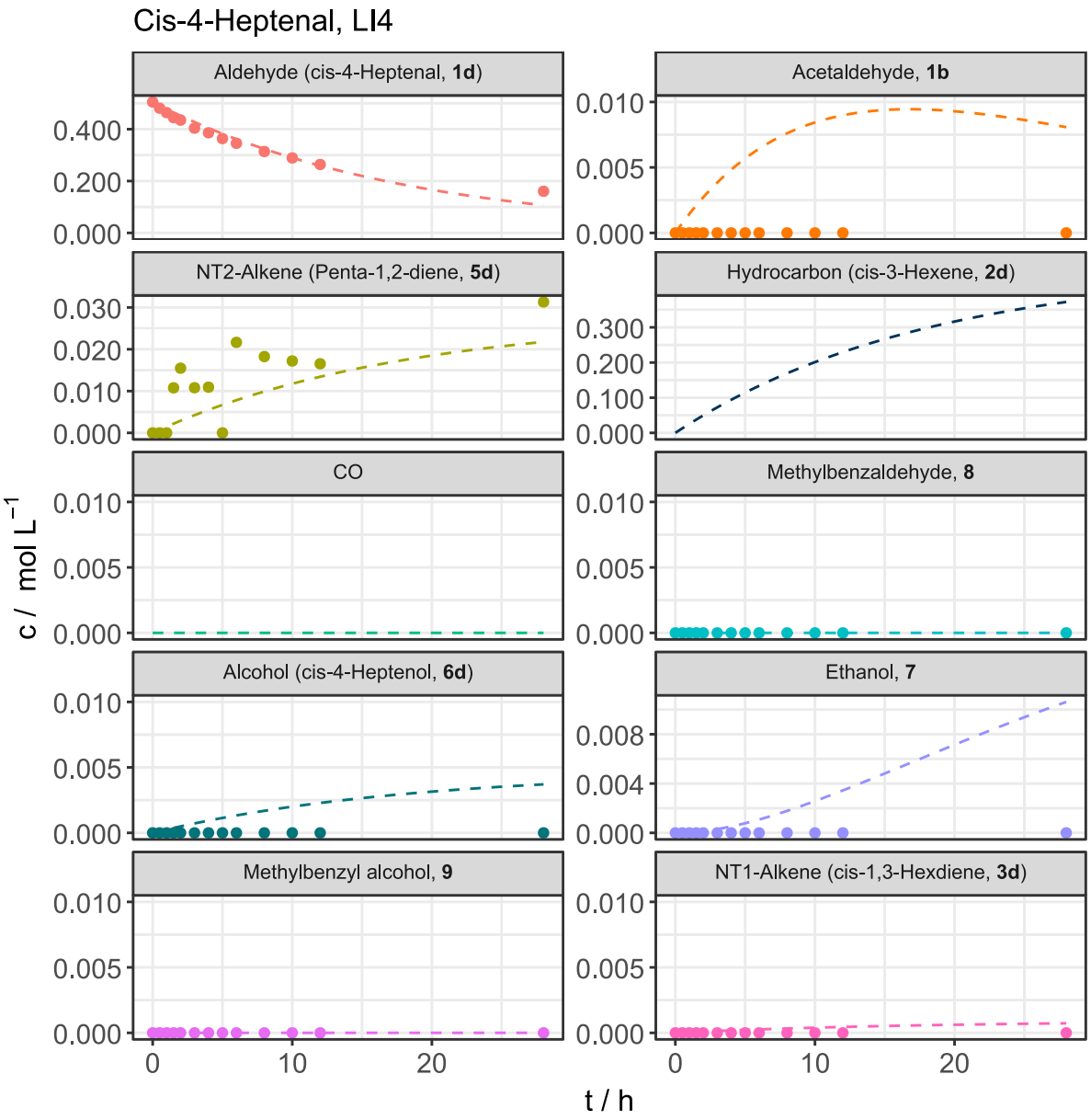

Figure S20. Concentration-time profiles for different species for the light-driven activation of cis-4-heptenal and the subsequent carbonylation of toluene at a photon flux density of 825.1 µmol m^{-2} s^{-1}.

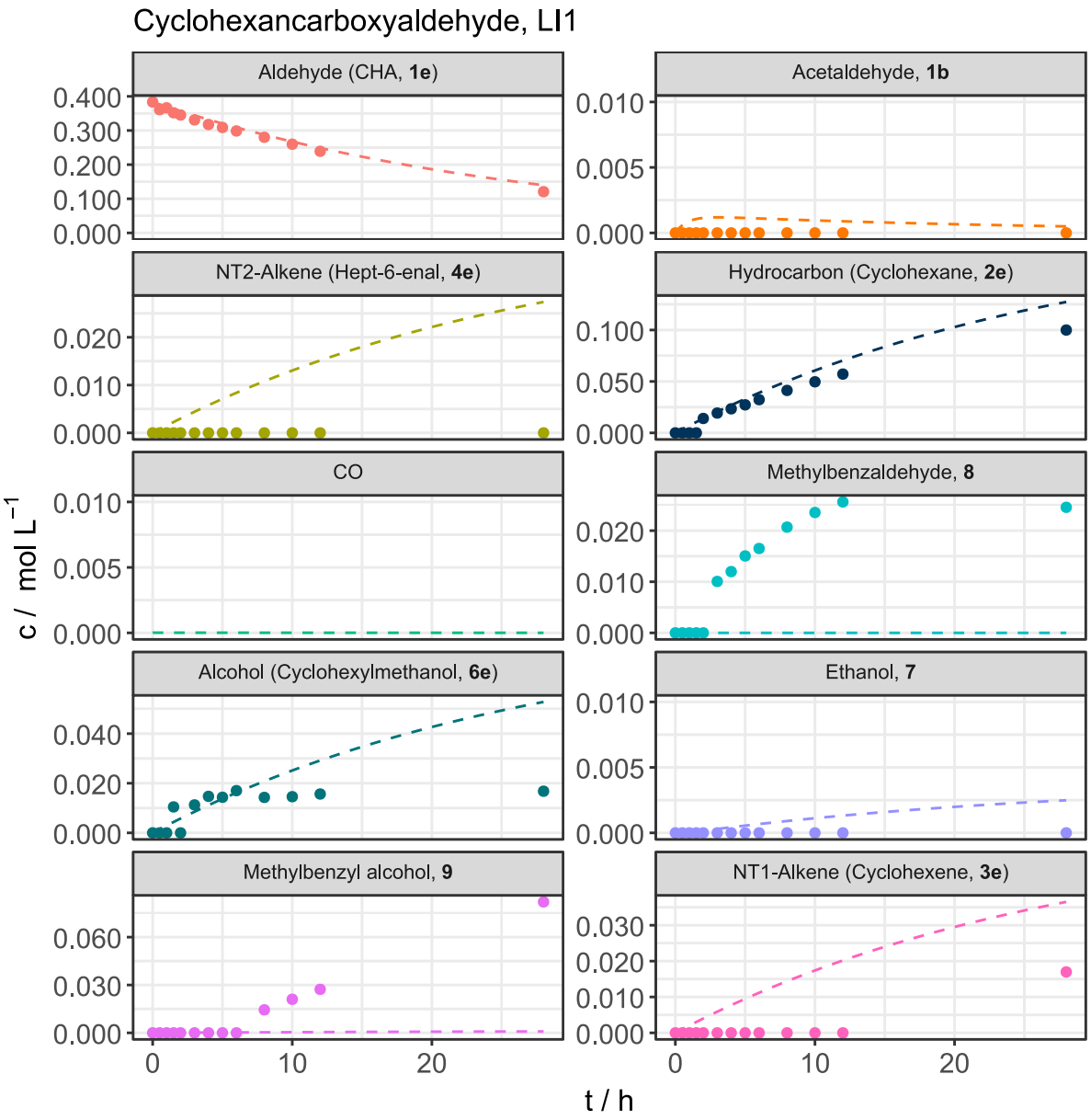

Figure S21. Concentration-time profiles for different species for the light-driven activation of cyclohexancarboxyaldehyde and the subsequent carbonylation of toluene at a photon flux density of 80.5 µmol m^{-2} s^{-1}.

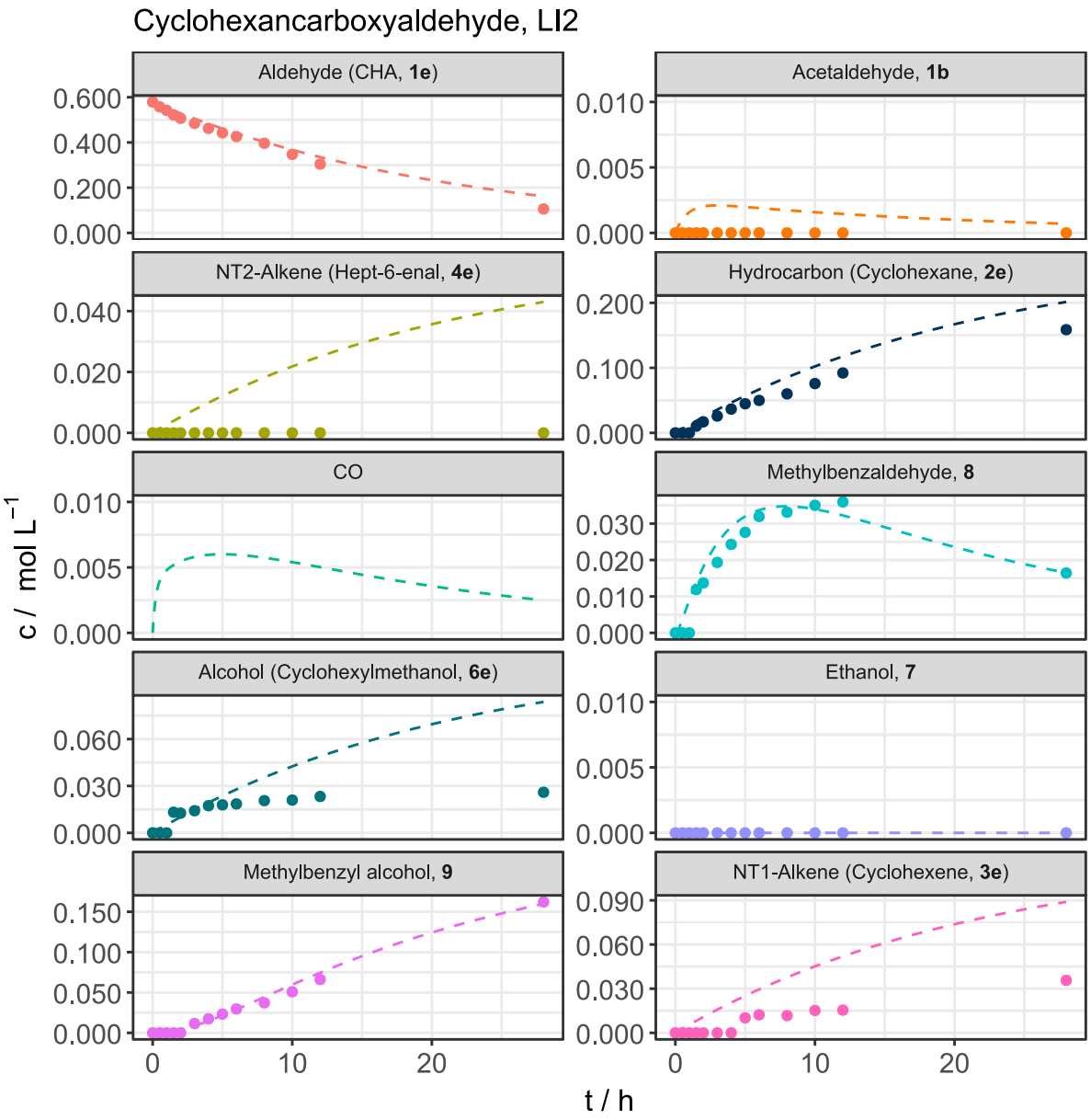

Figure S22. Concentration-time profiles for different species for the light-driven activation of cyclohexancarboxyaldehyde and the subsequent carbonylation of toluene at a photon flux density of 189.6 µmol m^{-2} s^{-1}.

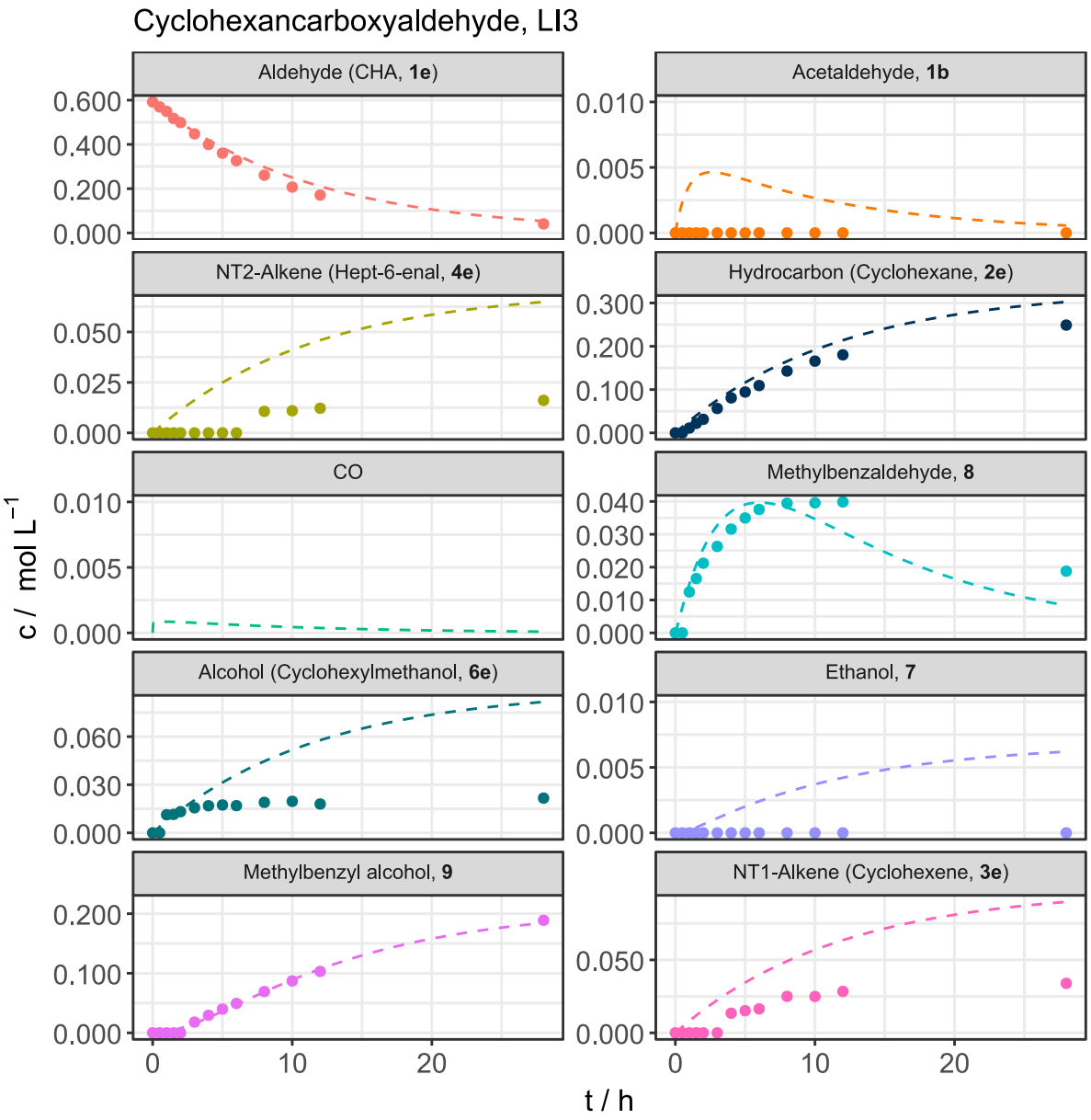

Figure S23. Concentration-time profiles for different species for the light-driven activation of cyclohexancarboxyaldehyde and the subsequent carbonylation of toluene at a photon flux density of 388.2 µmol m^{-2} s^{-1}.

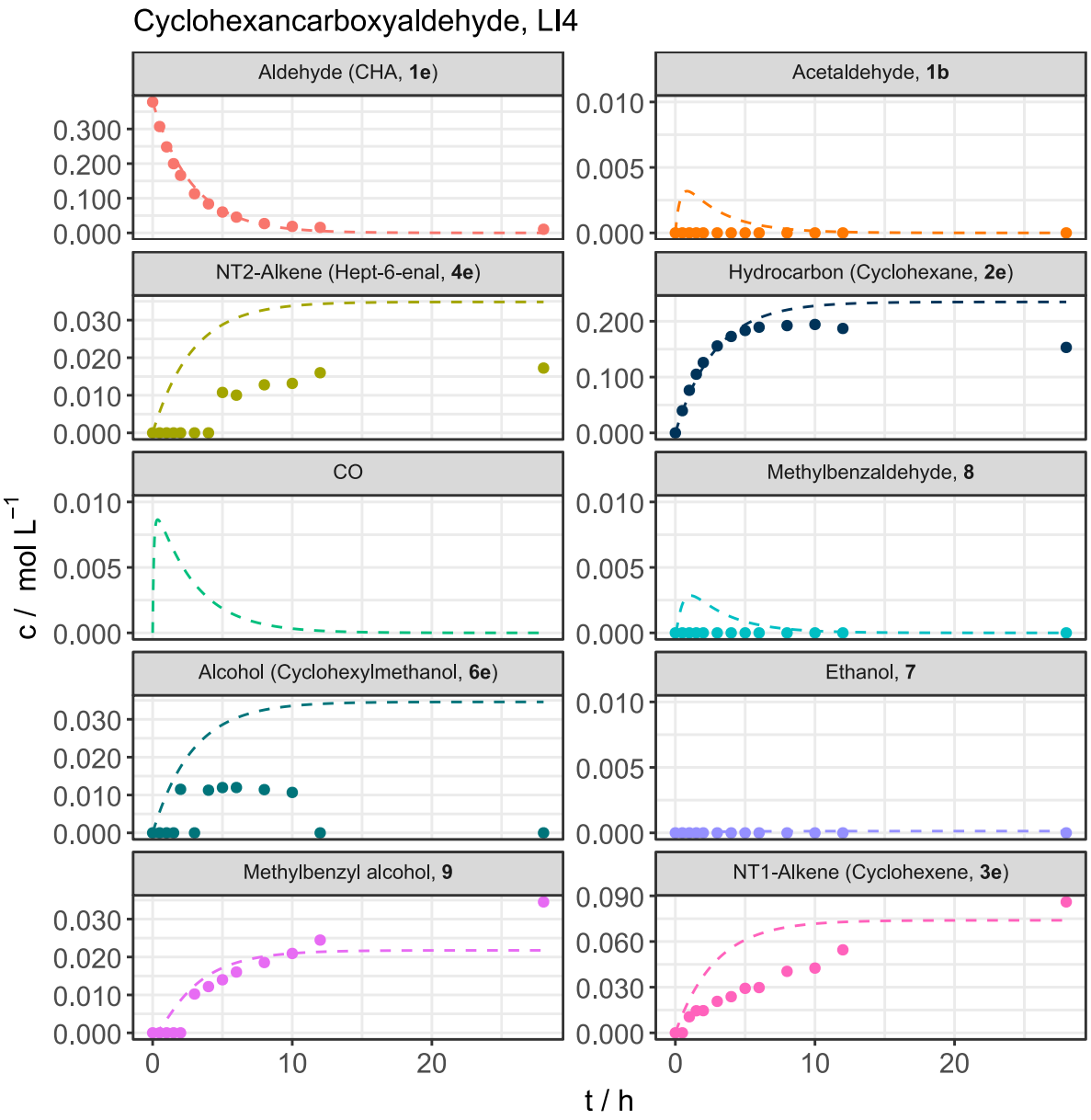

Figure S24. Concentration-time profiles for different species for the light-driven activation of cyclohexancarboxyaldehyde and the subsequent carbonylation of toluene at a photon flux density of 825.1 µmol m^{-2} s^{-1}.

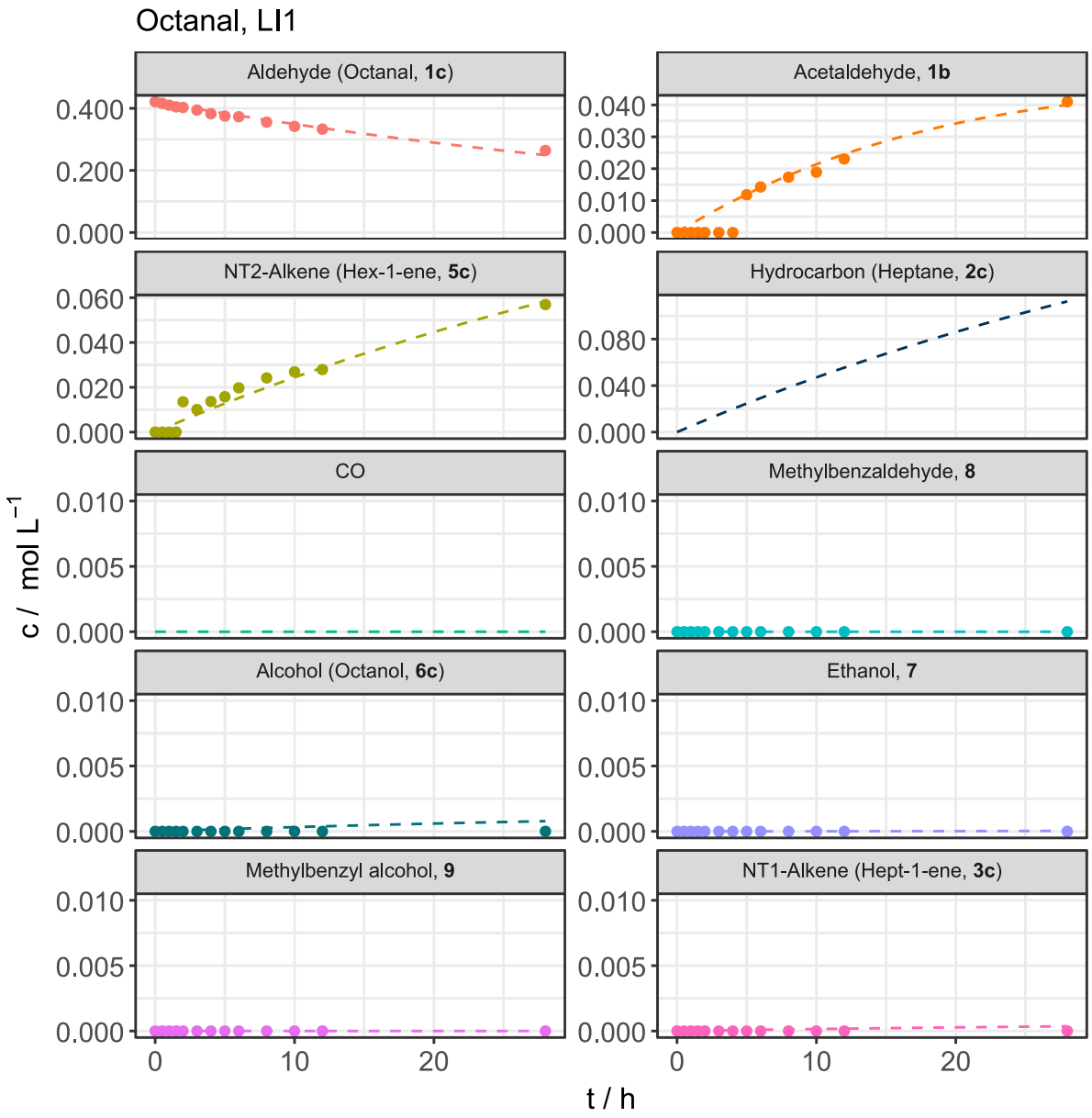

Figure S25. Concentration-time profiles for different species for the light-driven activation of octanal and the subsequent carbonylation of toluene at a photon flux density of 80.5 µmol m^{-2} s^{-1}.

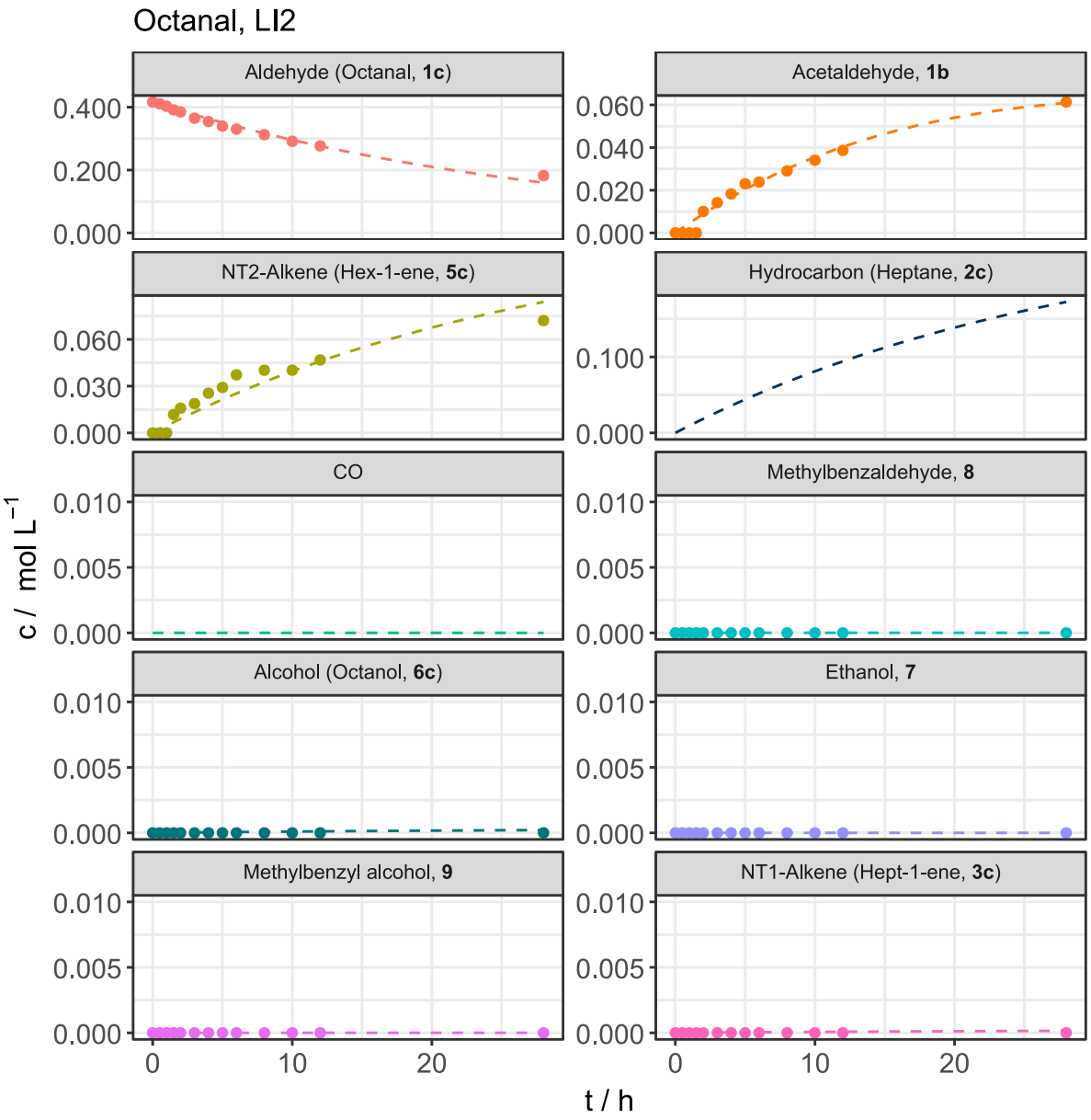

Figure S26. Concentration-time profiles for different species for the light-driven activation of octanal and the subsequent carbonylation of toluene at a photon flux density of 189.6 µmol m^{-2} s^{-1}.

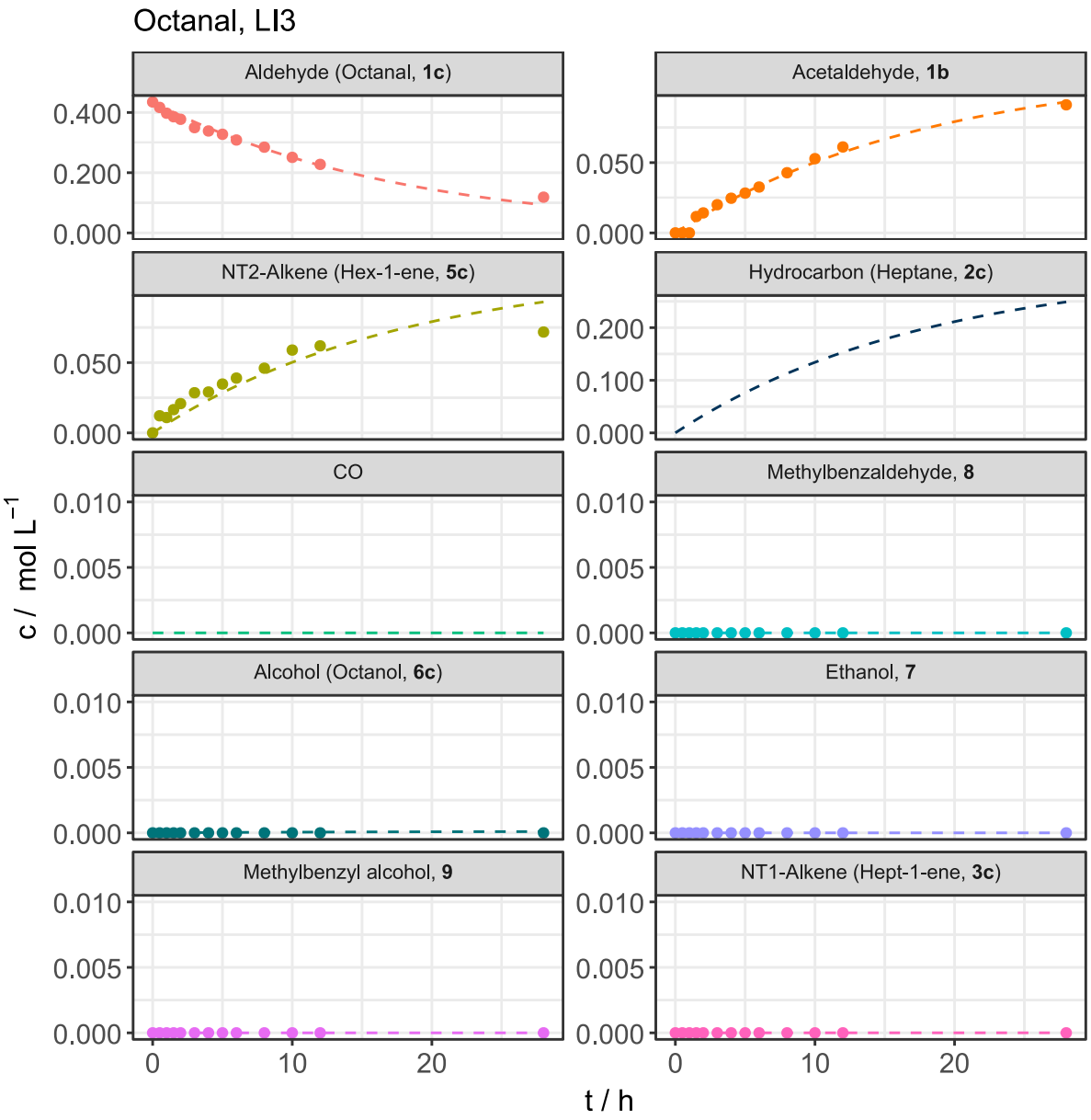

Figure S27. Concentration-time profiles for different species for the light-driven activation of octanal and the subsequent carbonylation of toluene at a photon flux density of 388.2 µmol m^{-2} s^{-1}.

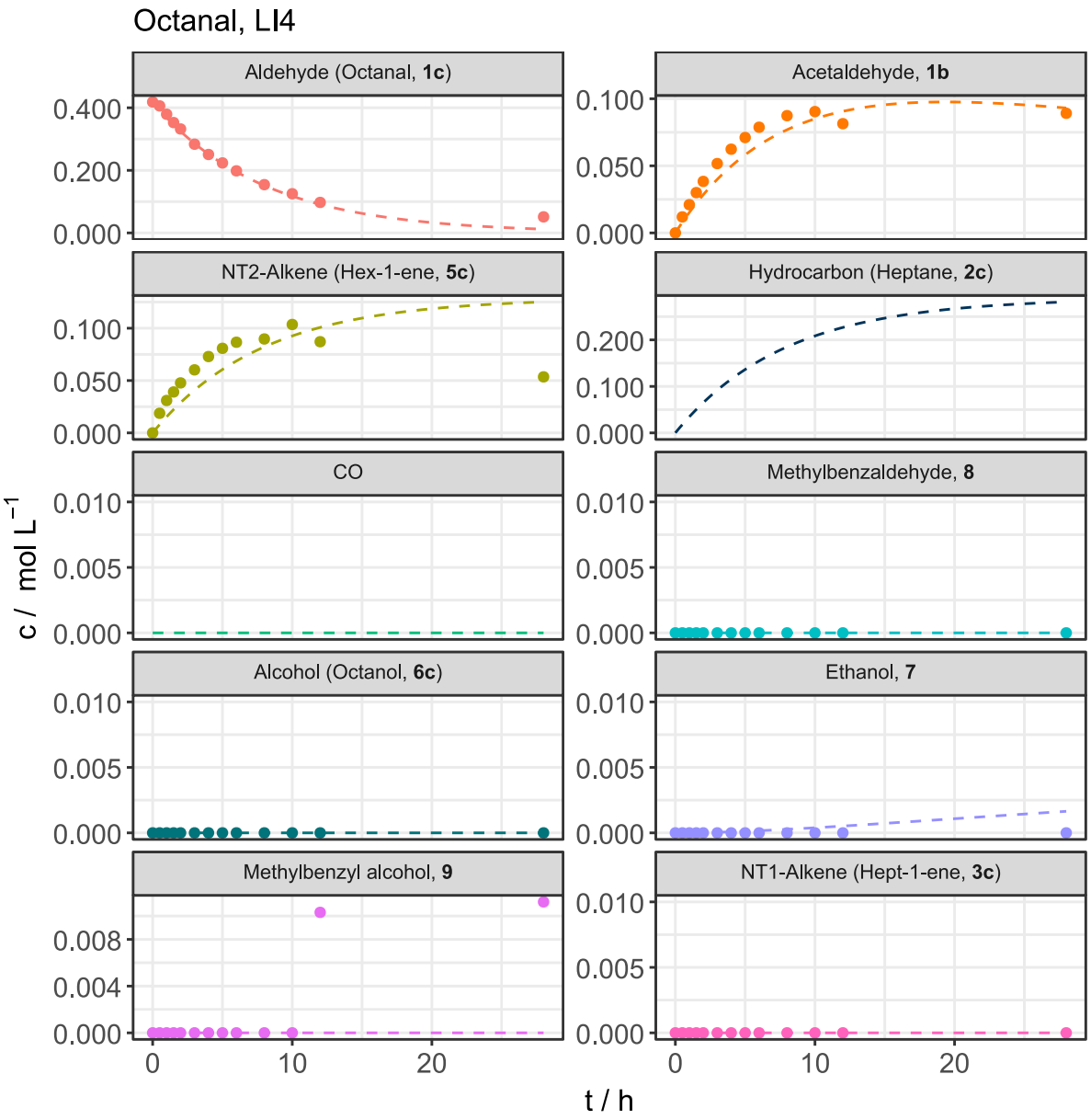

Figure S28. Concentration-time profiles for different species for the light-driven activation of octanal and the subsequent carbonylation of toluene at a photon flux density of 825.1 µmol m^{-2} s^{-1}.

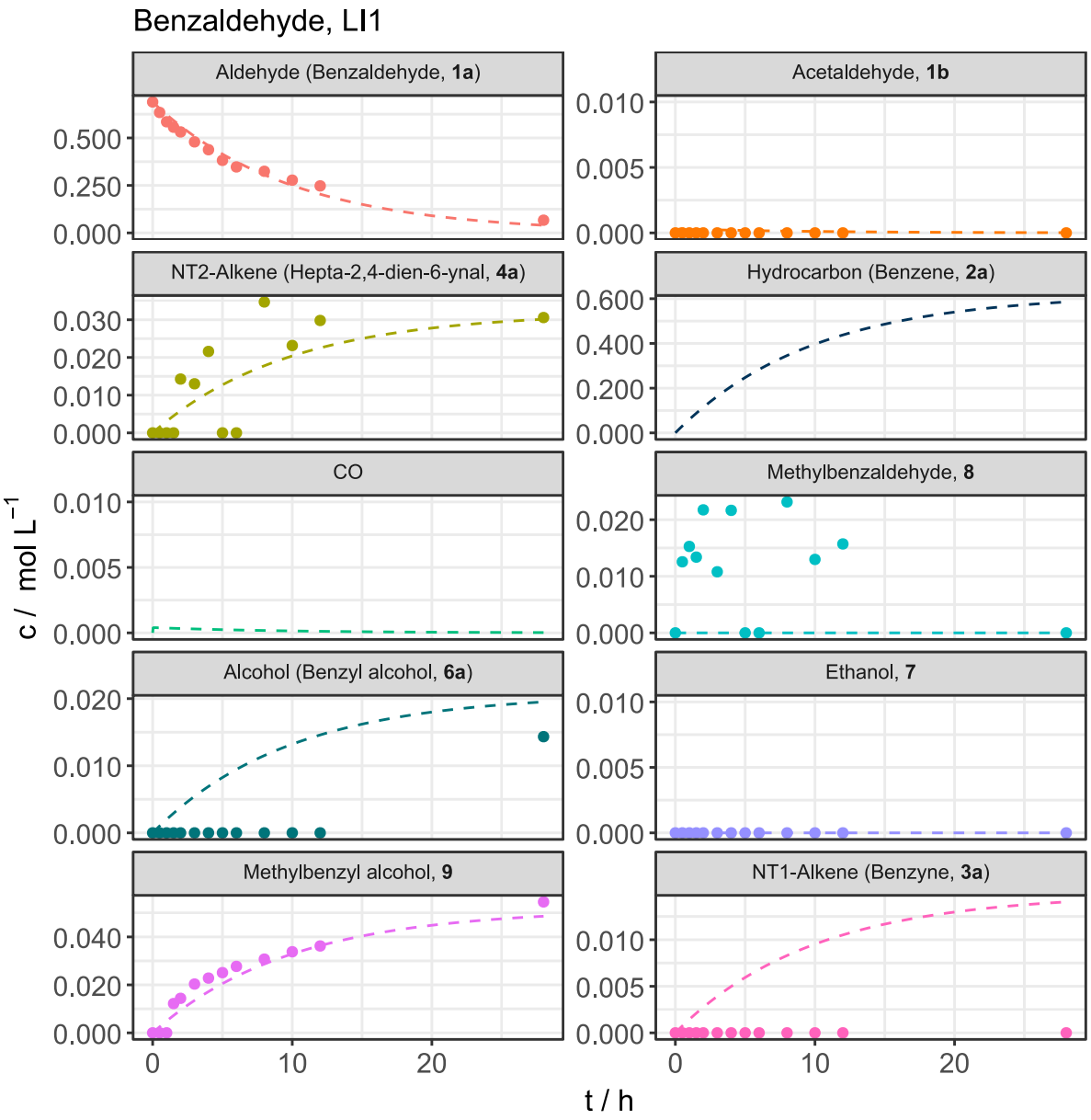

Figure S29. Concentration-time profiles for different species for the light-driven activation of benzaldehyde and the subsequent carbonylation of toluene with no C-H activation catalyst present at a photon flux density of 80.5 µmol m^{-2} s^{-1}.

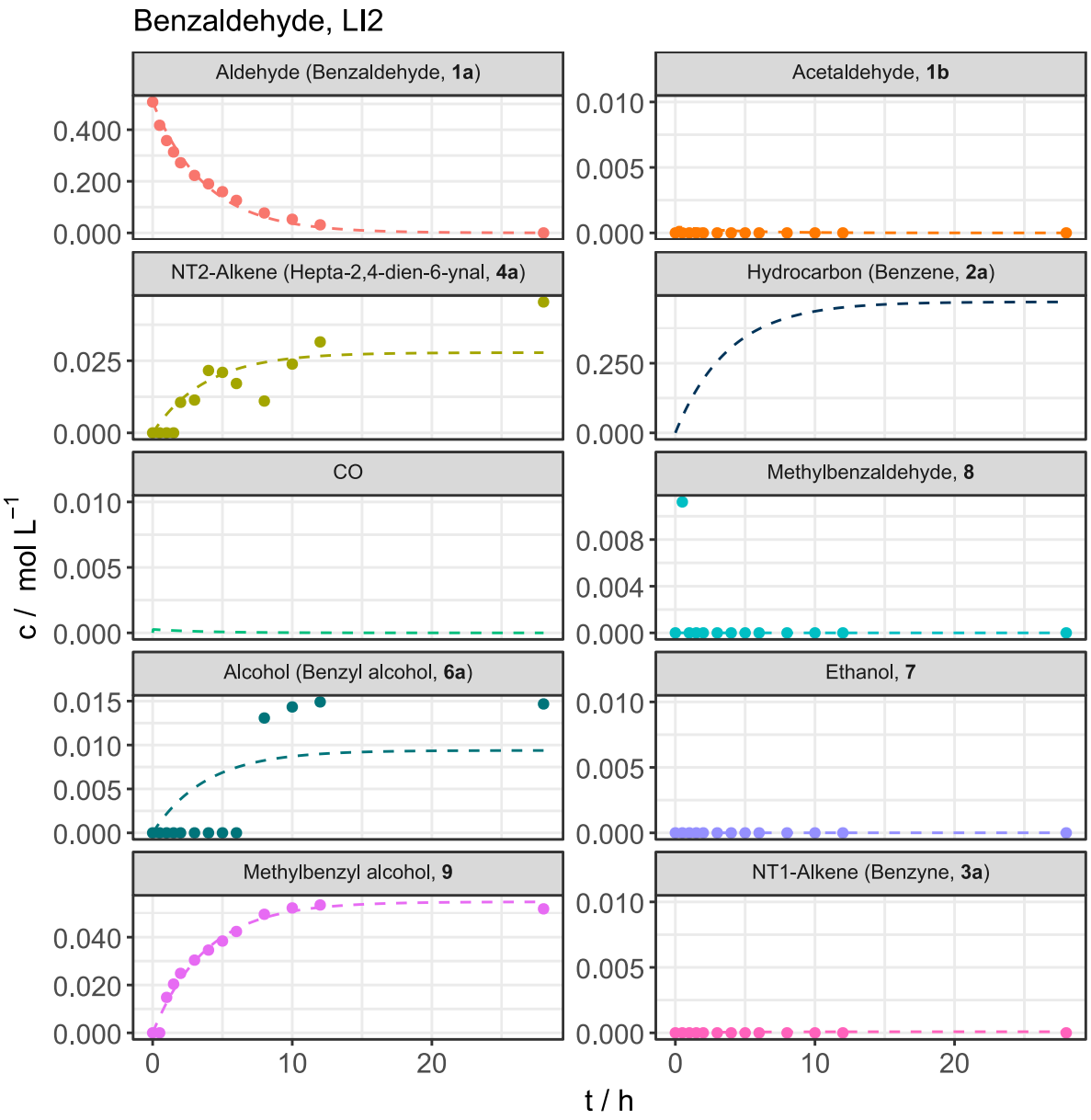

Figure S30. Concentration-time profiles for different species for the light-driven activation of benzaldehyde and the subsequent carbonylation of toluene with no C-H activation catalyst present at a photon flux density of 189.6 µmol m^{-2} s^{-1}.

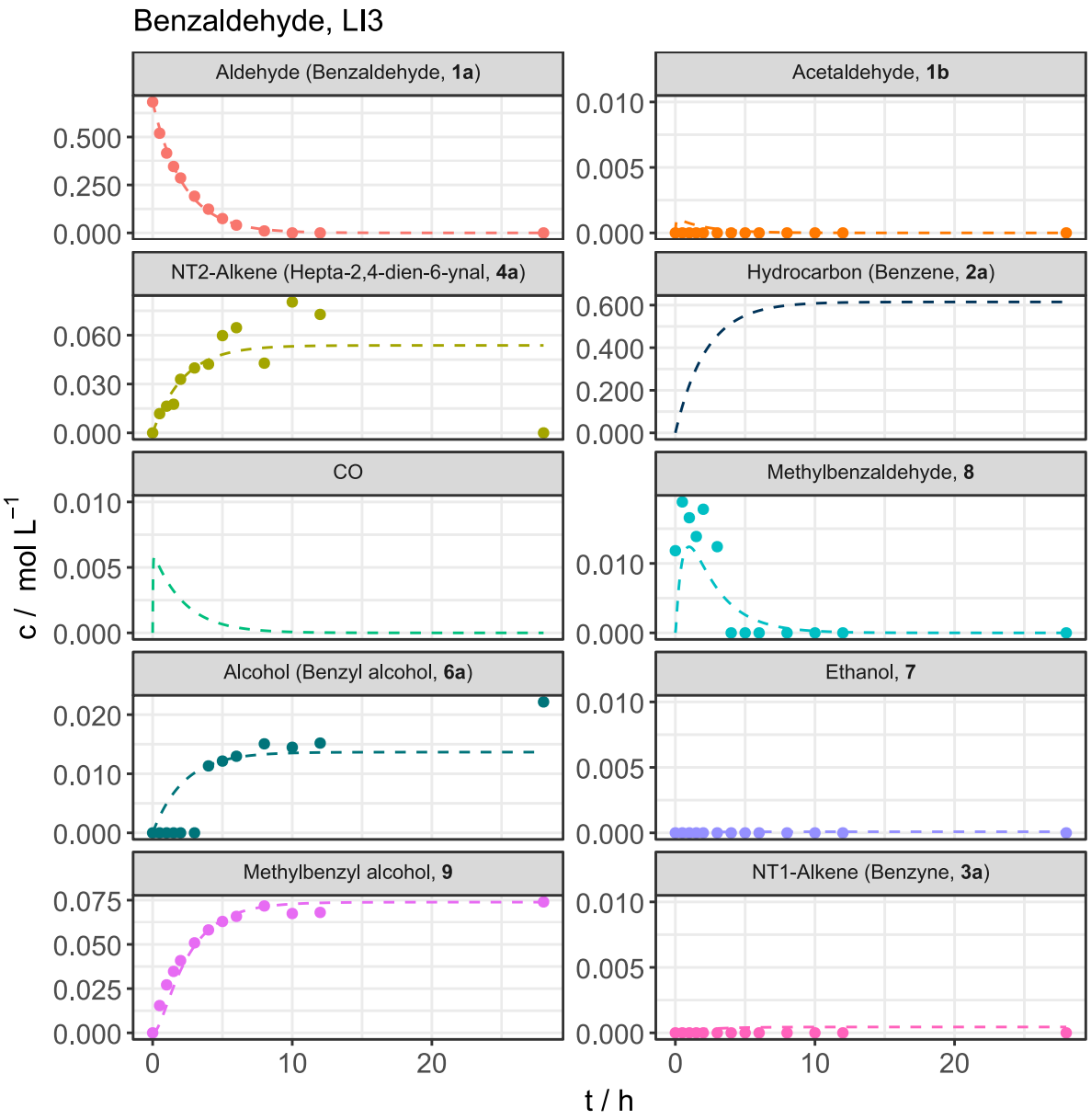

Figure S31. Concentration-time profiles for different species for the light-driven activation of benzaldehyde and the subsequent carbonylation of toluene with no C-H activation catalyst present at a photon flux density of 388.2 µmol m^{-2} s^{-1}.

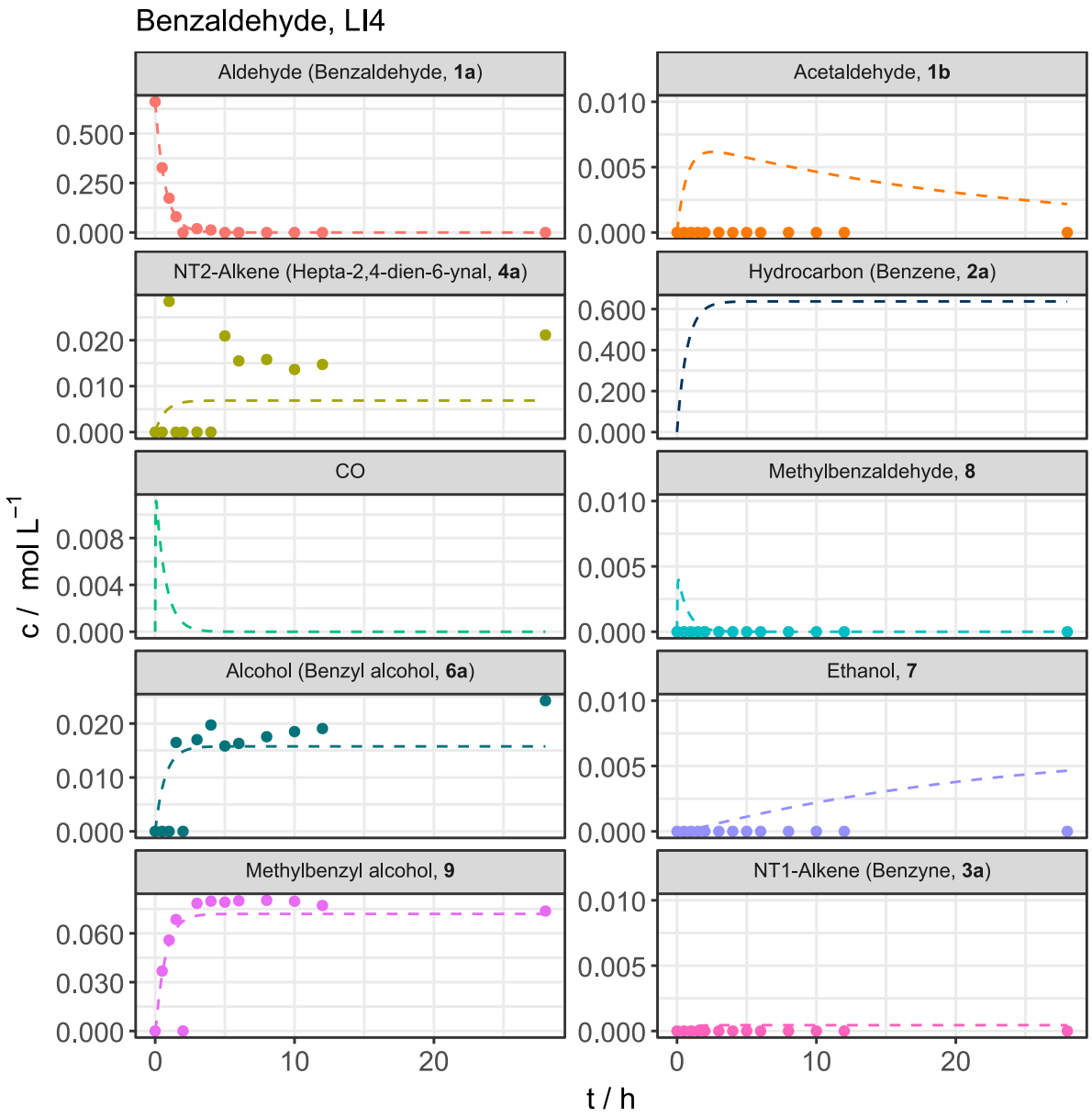

Figure S32. Concentration-time profiles for different species for the light-driven activation of benzaldehyde and the subsequent carbonylation of toluene with no C-H activation catalyst present at a photon flux density of 825.1 µmol m^{-2} s^{-1}.

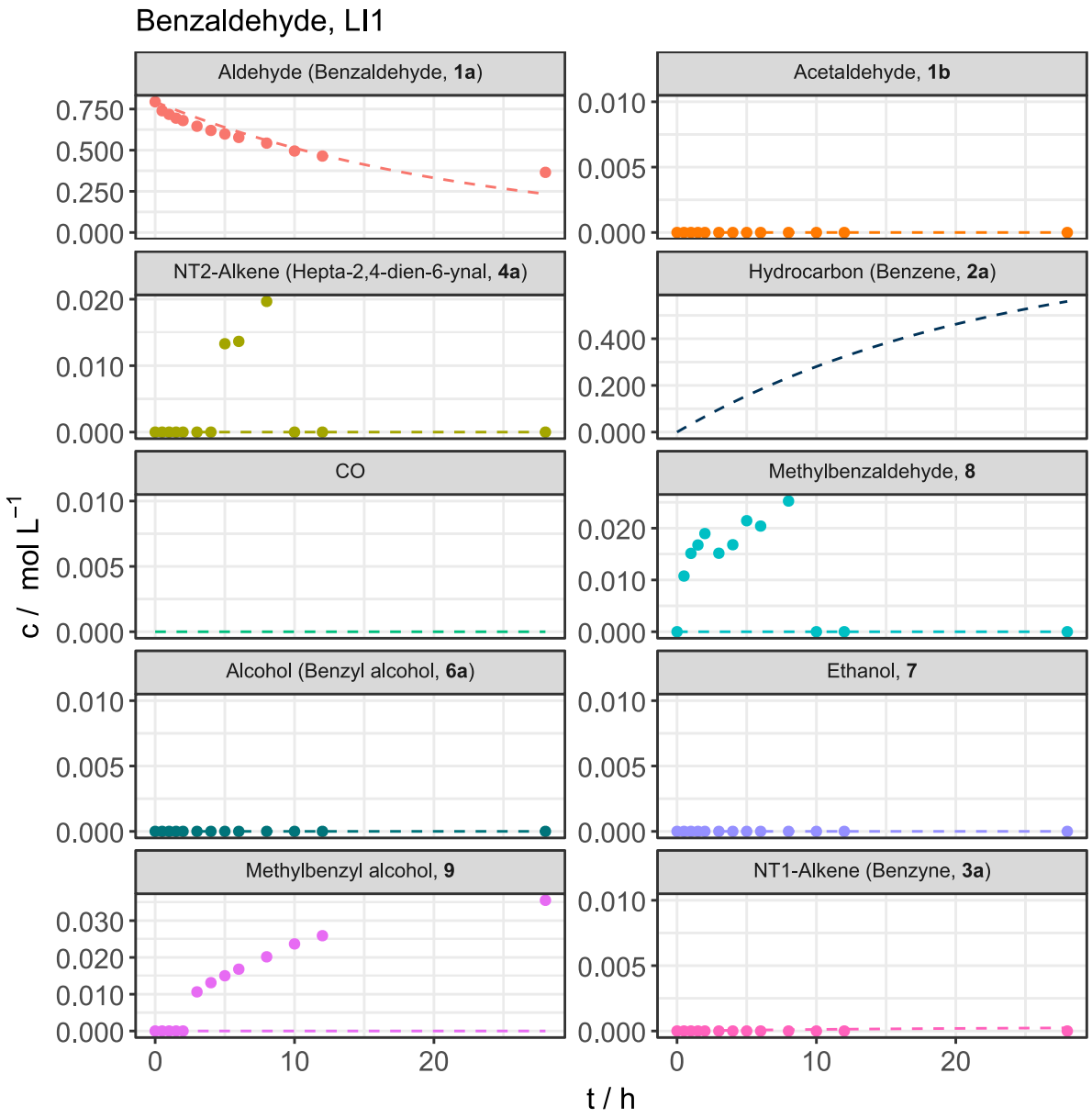

Figure S33. Concentration-time profiles for different species for the light-driven activation of benzaldehyde and the subsequent carbonylation of toluene with no C-H activation catalyst present at a photon flux density of 80.5 µmol m^{-2} s^{-1}. The irradiation took place through an 8 mm window glass block.

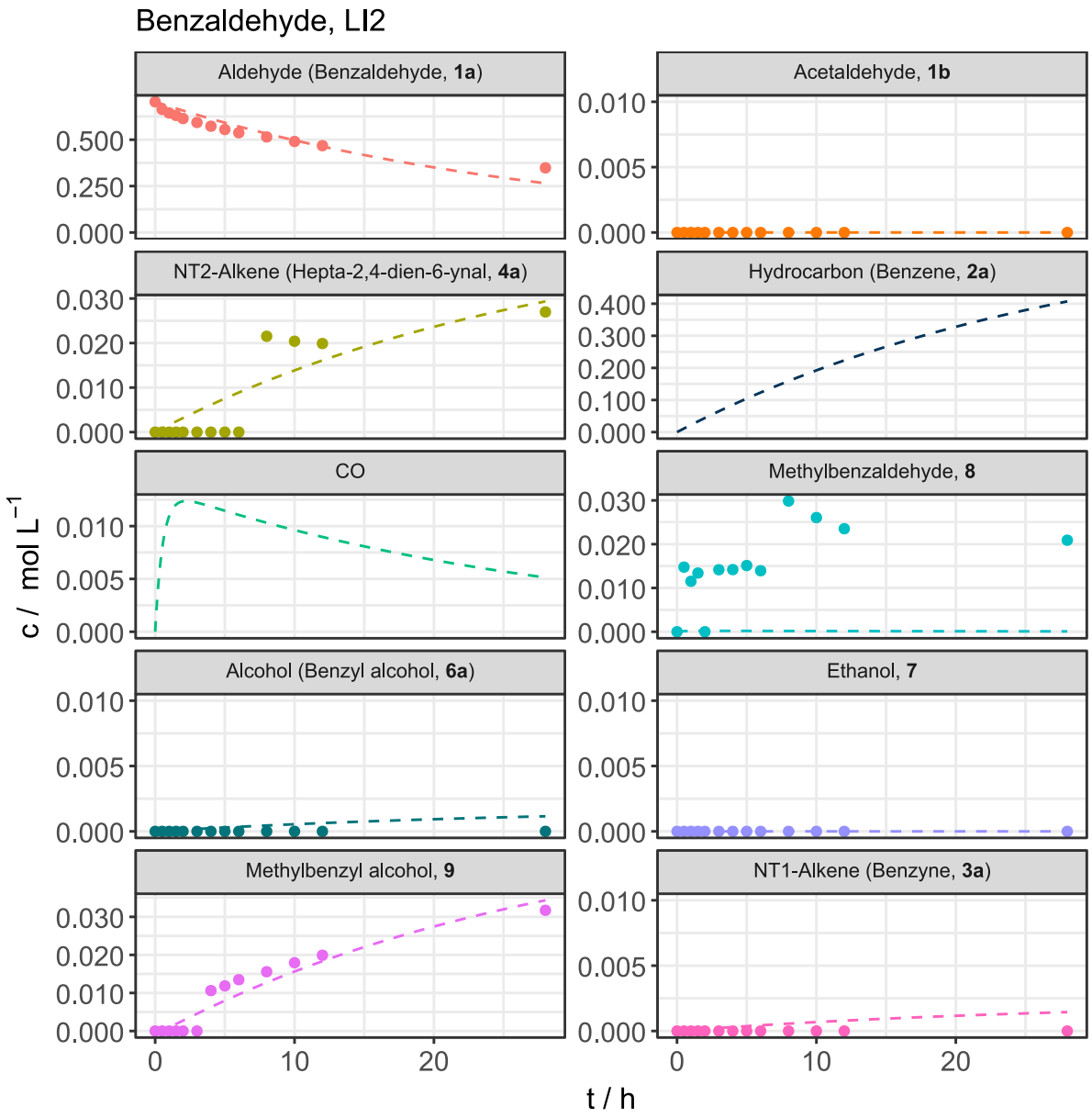

Figure S34. Concentration-time profiles for different species for the light-driven activation of benzaldehyde and the subsequent carbonylation of toluene with no C-H activation catalyst present at a photon flux density of 189.6 µmol m^{-2} s^{-1}. The irradiation took place through an 8 mm window glass block.

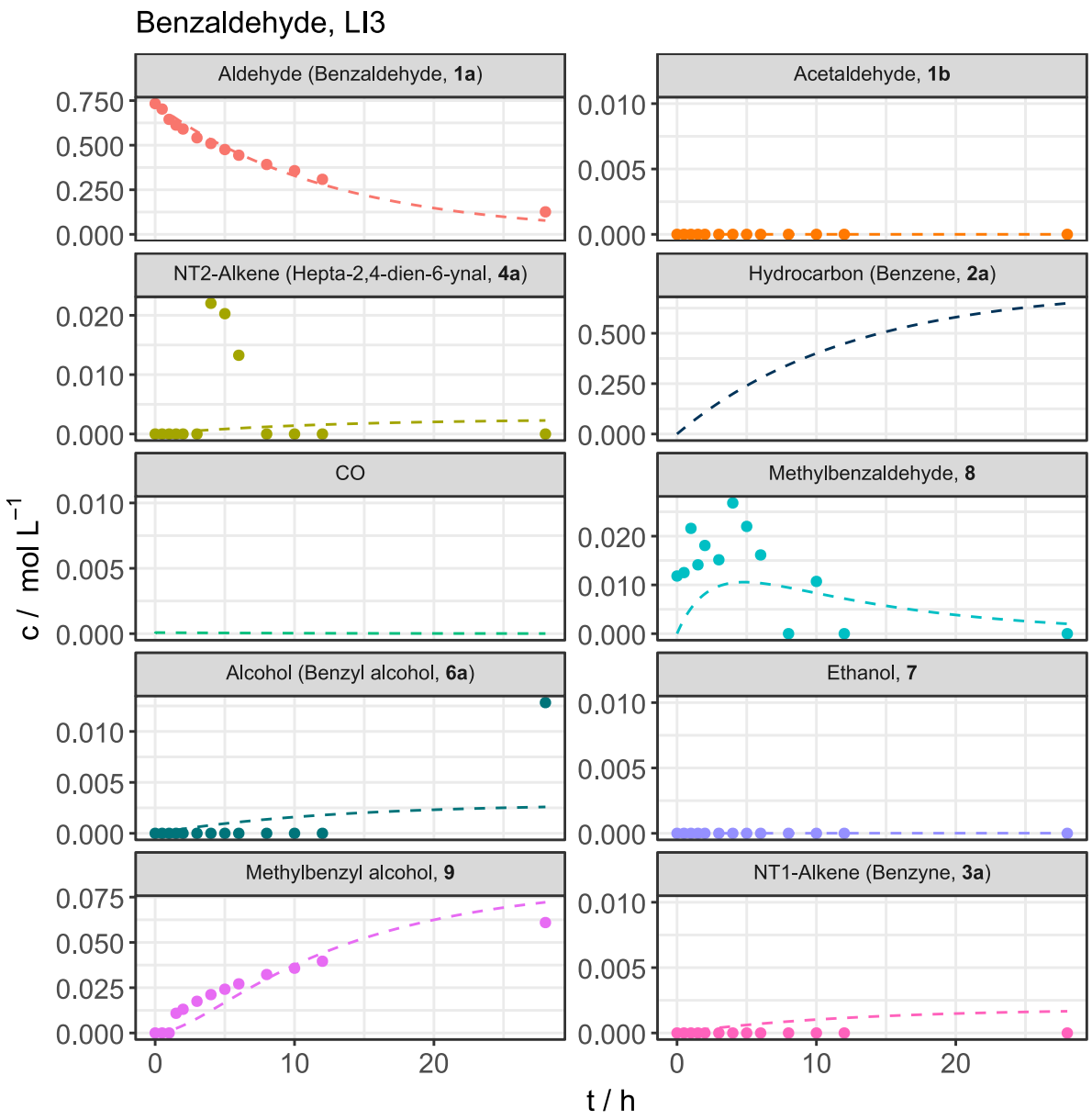

Figure S35. Concentration-time profiles for different species for the light-driven activation of benzaldehyde and the subsequent carbonylation of toluene with no C-H activation catalyst present at a photon flux density of 388.2 µmol m^{-2} s^{-1}. The irradiation took place through an 8 mm window glass block.

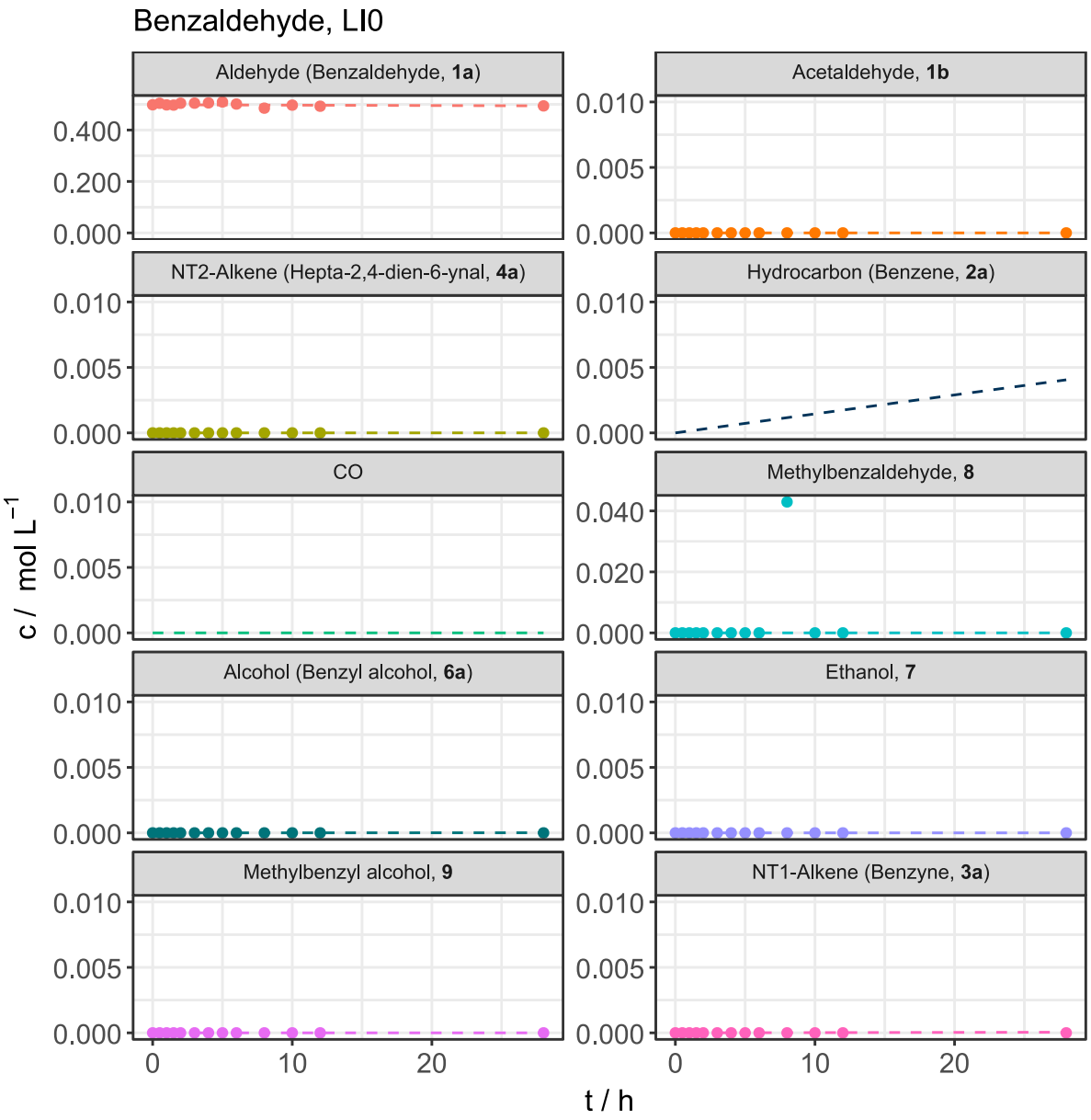

Figure S36. Concentration-time profiles for different species for the thermal activation of benzaldehyde at 50 °C.

4. Additional NMR Spectra

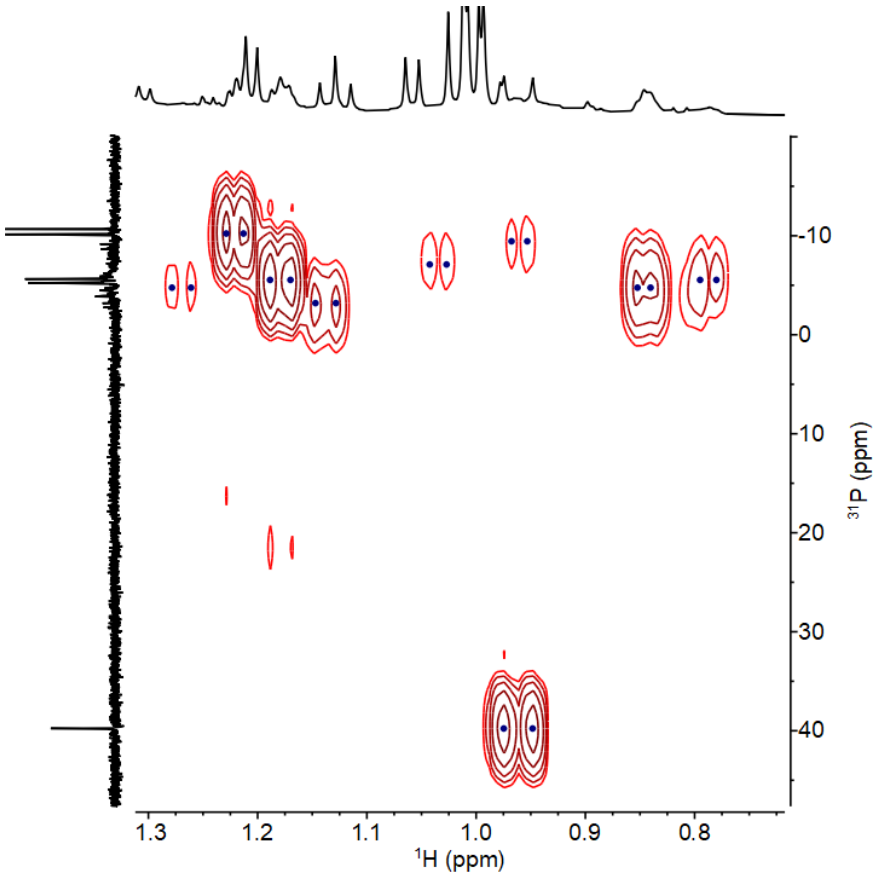

Figure S37. ^{1}H-^{31}P-HMBC spectrum after 240 minutes for the light-driven activation of acetaldehyde and the subsequent carbonylation of toluene at a photon flux density of 189.6 µmol m^{-2} s^{-1}.

5. DFT-Calculated NMR Shifts and $^1J_{Rh,P}$ Coupling Constants

Table S2. DFT calculated ^{31}P NMR shifts and $^1J_{Rh,P}$ coupling constants for different Rh-phosphine complexes. All calculations were done with benzene as an implicit solvent. The shifts were referenced to H_3PO_4 and corrected by dividing by a factor of 1.073.

Complex	δ(P1)	δ(P2)	δ(P3)	δ(P4)	$^1J_{Rh,P1}$	$^1J_{Rh,P2}$	$^1J_{Rh,P3}$	$^1J_{Rh,P4}$
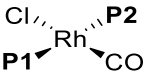	-9.7	-9.7	-	-	-157	-157	-	-
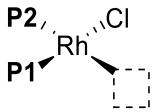	20.9	87.3	-	-	-268	-286	-	-
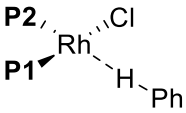	21.8	57.4	-	-	-303	-409	-	-
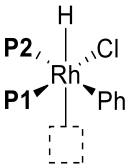	-19.8	23.6	-	-	-101	-234	-	-
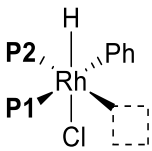	-15.0	89.7	-	-	-126	-321	-	-
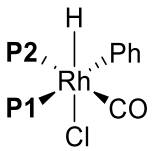	-12.0	-3.4	-	-	-111	-155	-	-
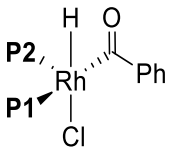	-17.0	70.2	-	-	-119	-353	-	-
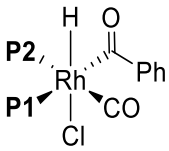	-20.2	-1.2	-	-	-186	-65	-	-
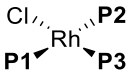	-3.8	-5.9	15.2	-	-185	-190	-262	-
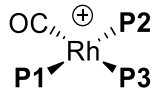	-12.4	-12.7	-22.2	-	-150	-151	-172	-
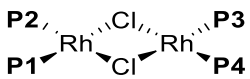	23.9	23.4	23.5	23.9	-323	-317	-317	-323
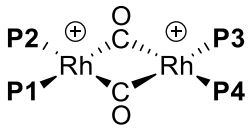	-6.6	-7.6	15.0	59.1	-233	-193	-276	-292
	231.6	231.6	-	-	-118	-141	-141*	-118*

*$^1J_{Rh1,P2}$ and $^1J_{Rh2,P1}$, respectively

6. UV/Vis spectra

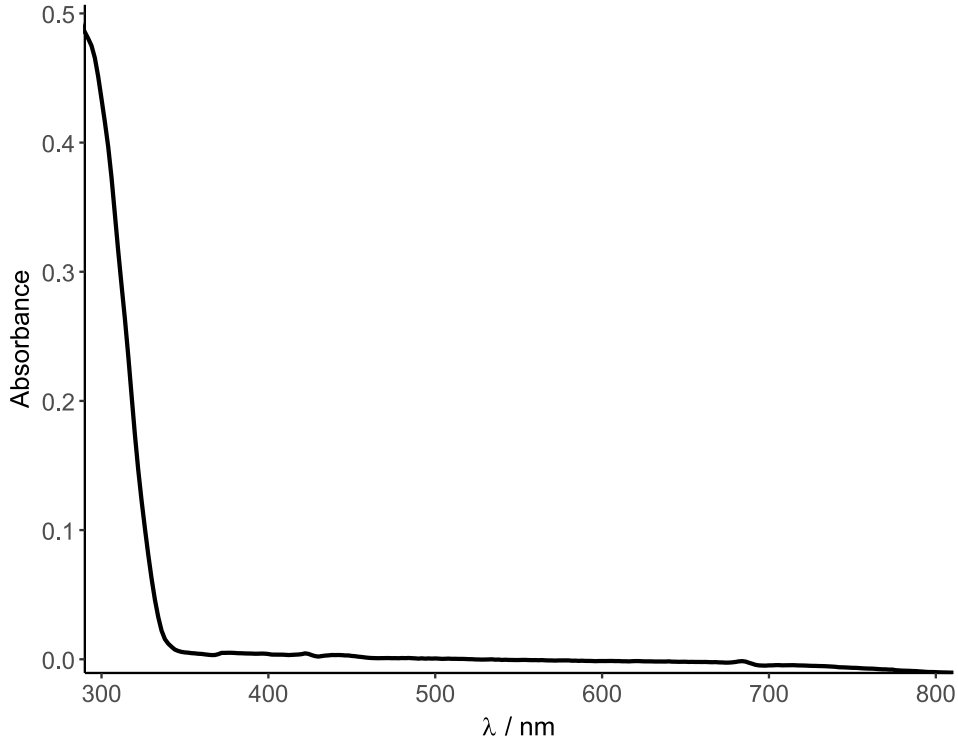

Figure S38. UV/Vis absorption spectrum of acetaldehyde in toluene.

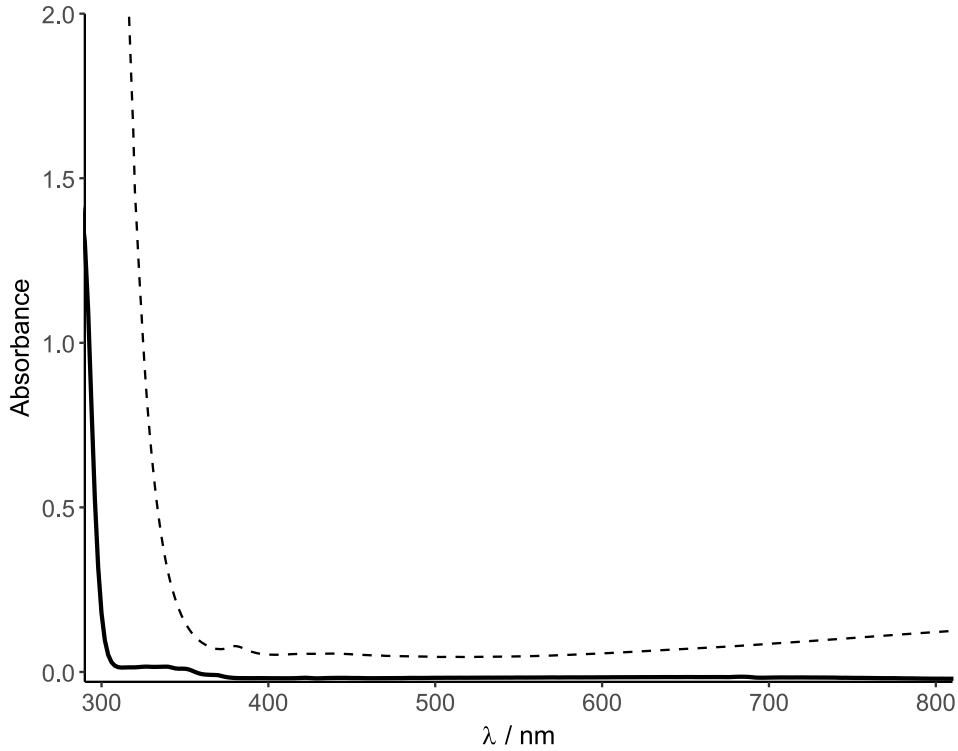

Figure S39. UV/Vis absorption spectrum of benzaldehyde in toluene. The dashed line indicates the absorption spectrum of the 8 mm window glass.

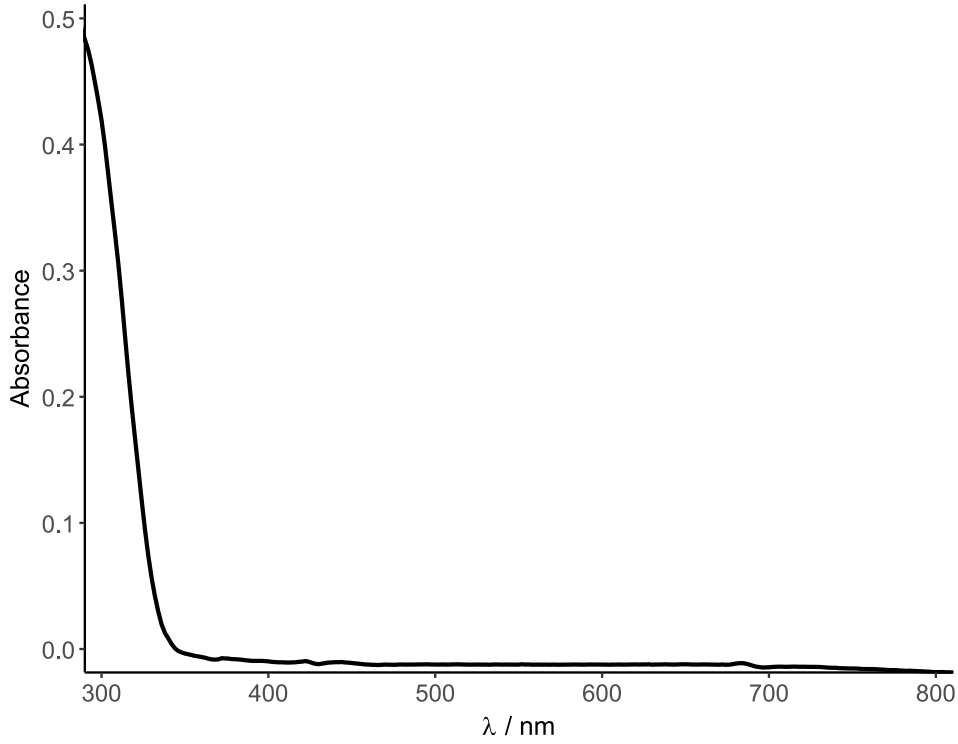

Figure S40. UV/Vis absorption spectrum of cis-4-heptenal in toluene.

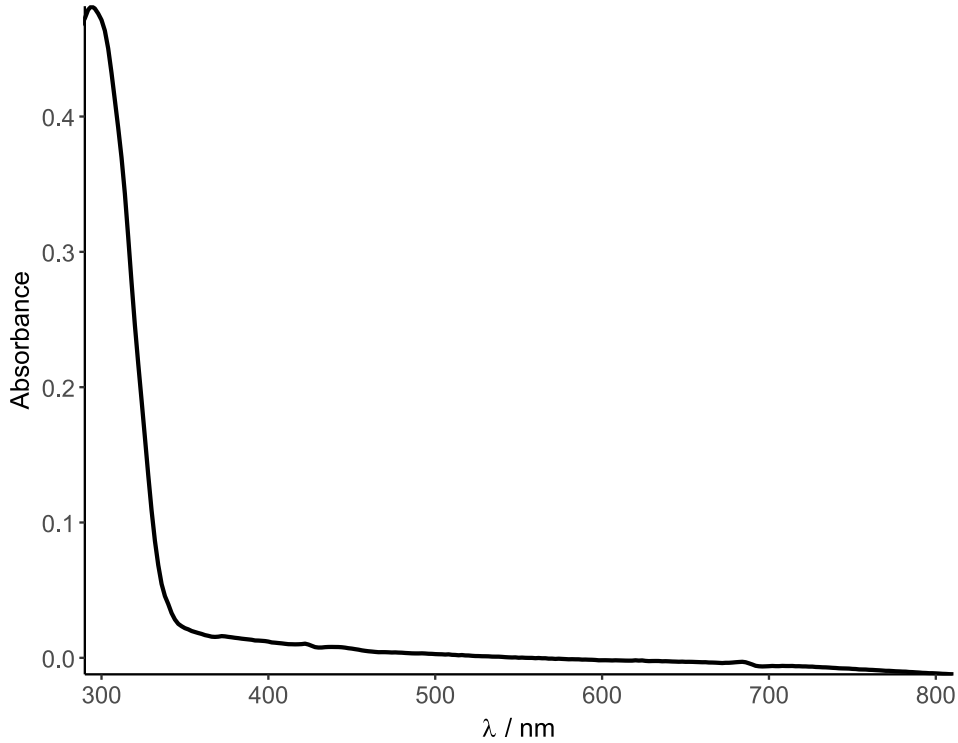

Figure S41. UV/Vis absorption spectrum of cyclohexylcarbaldehyde in toluene.

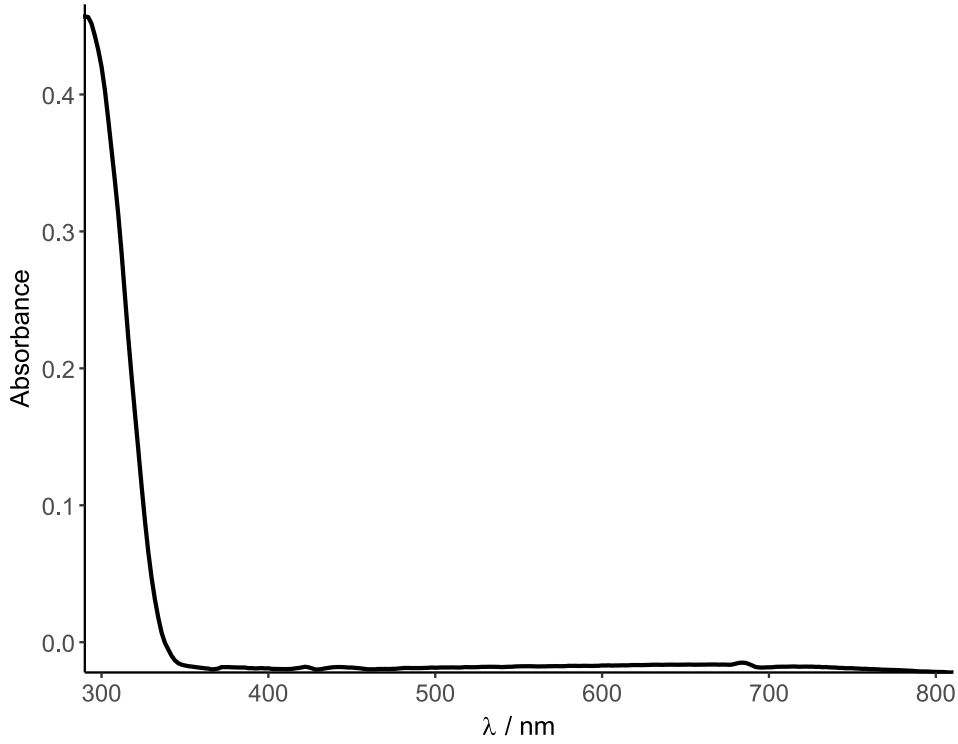

Figure S42. UV/Vis absorption spectrum of octanal in toluene.

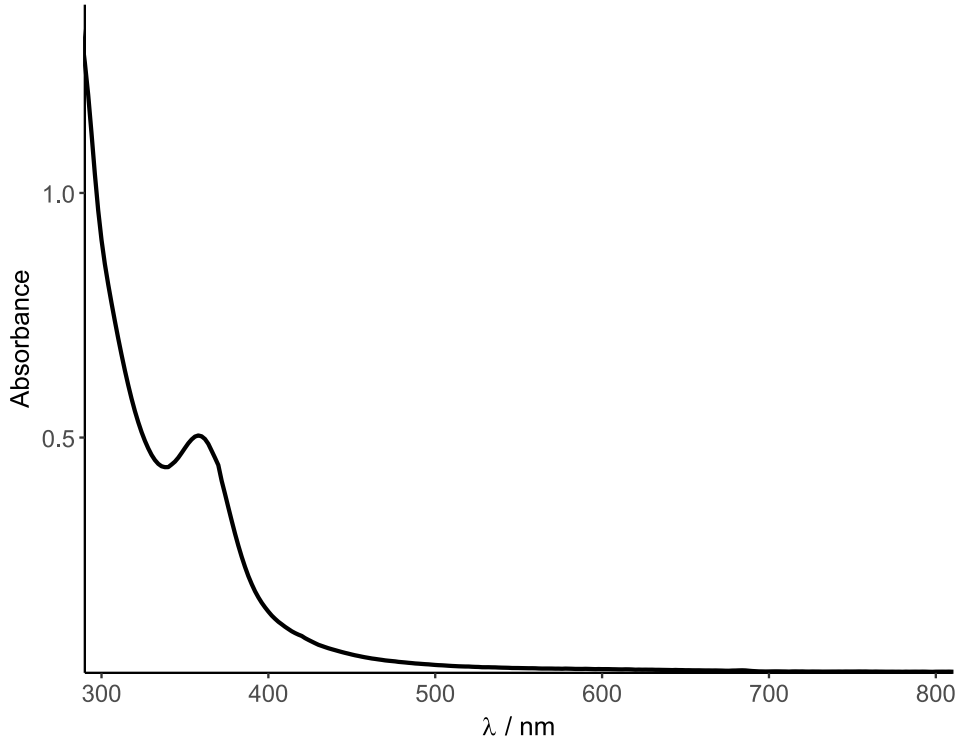

Figure S43. UV/Vis absorption spectrum of [Rh(Cl)(CO)(PMe_3)$_2$] in toluene.

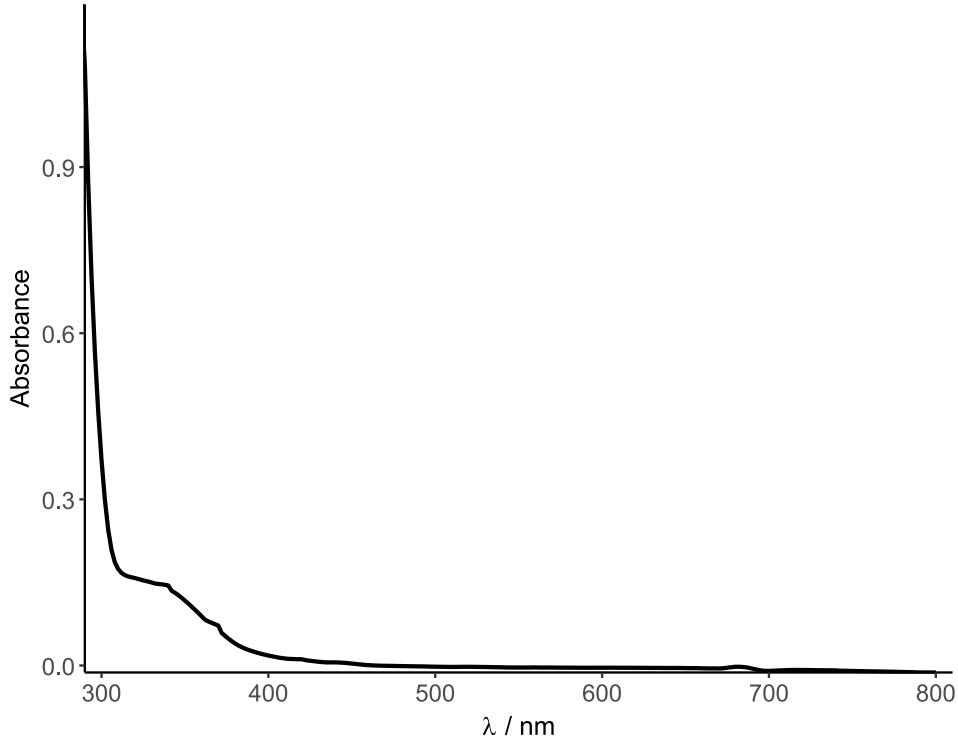

Figure S44. UV/Vis absorption spectrum of the diluted reaction mixture containing benzaldehyde and [Rh(Cl)(CO)(PMe_3)$_2$] in toluene (1:2500).